COVER

Link :
https://link.springer.com/journal/42461/volumes-and-issues/41-3

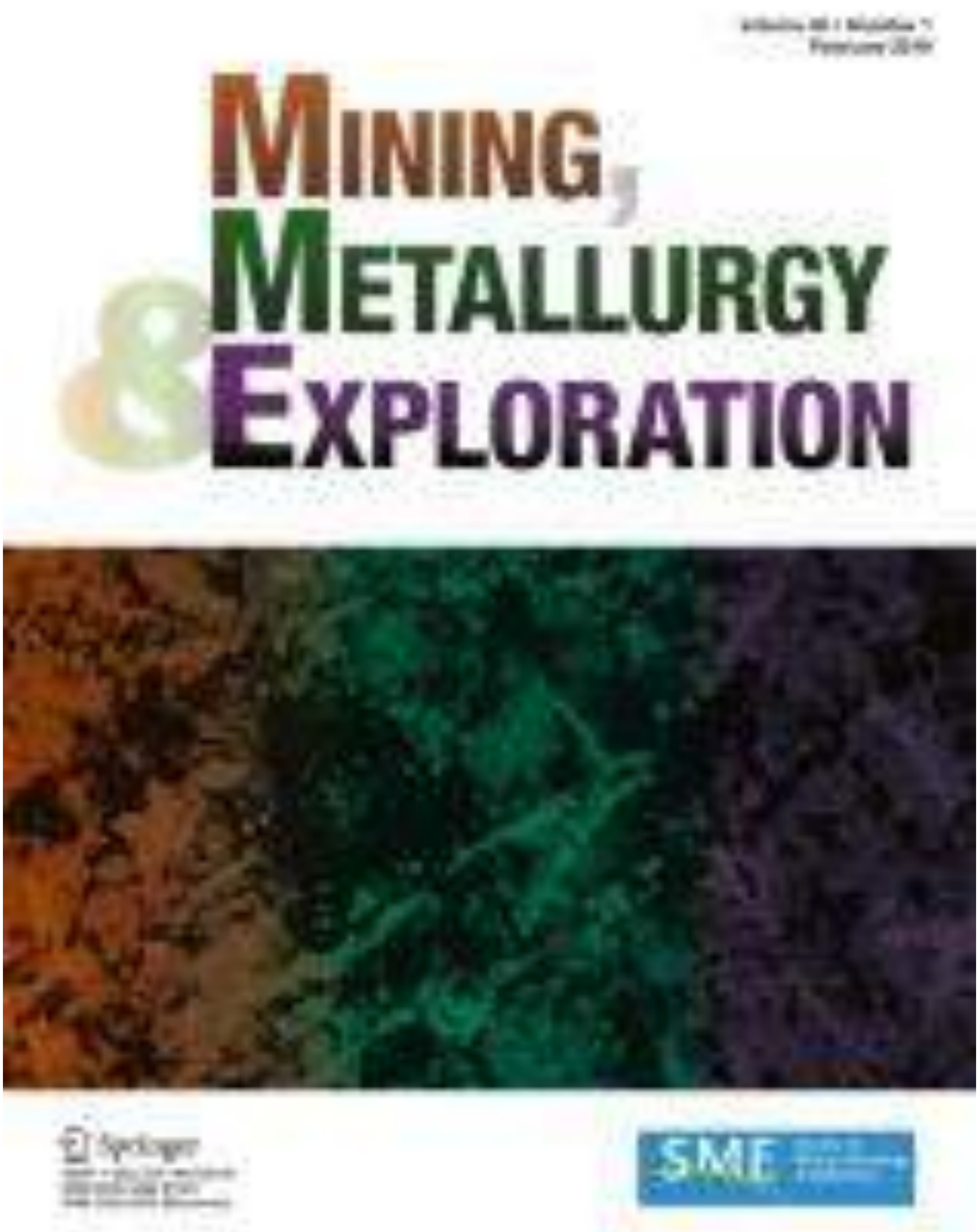

CONTENTS

Link :
https://link.springer.com/journal/42461/volumes-and-issues/41-3

EDITORIAL BOARD/COMMITTEE

Link :
https://link.springer.com/journal/42461/editors

E-ISSN : 2524-3470
P-ISSN : 2524-3462

Link :
https://portal.issn.org/resource/ISSN/2524-3470

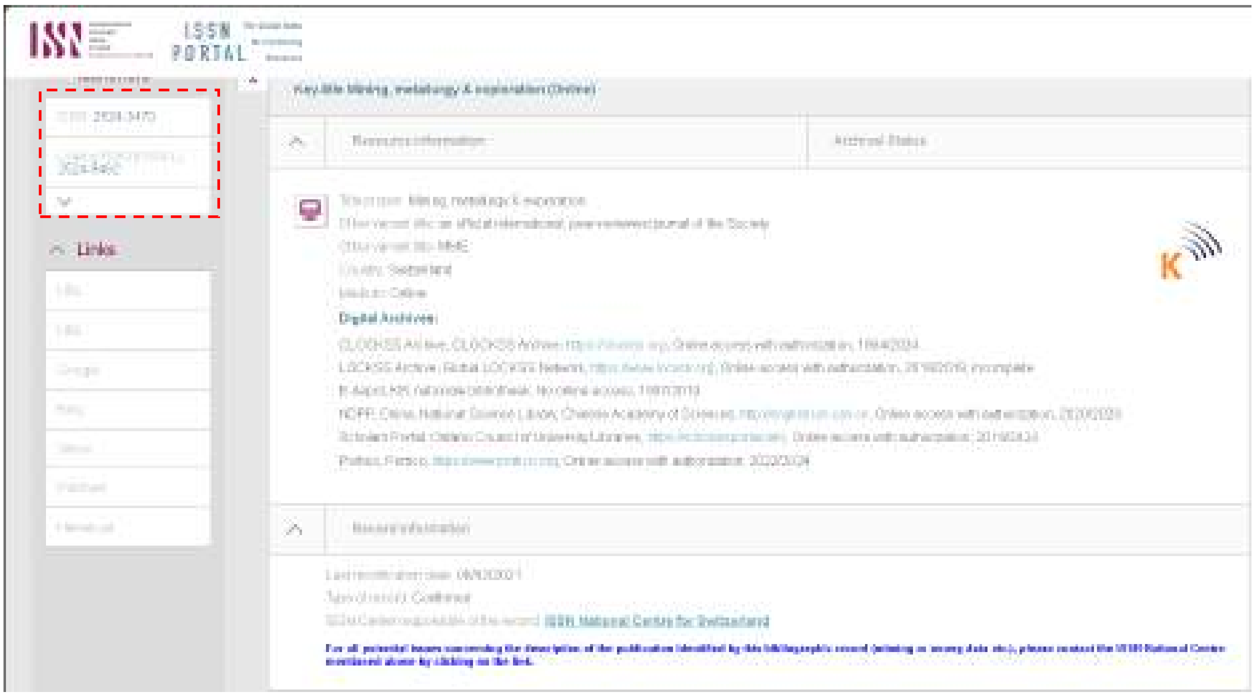

Scopus : Q2
SJR (2023) : 0,397
Impact Factor (2023) : 1,5
Impact Factor 5-tahun : 1,8

Link ISSN :
https://portal.issn.org/resource/ISSN/2524-3470
Link Scimago :
https://www.scimagojr.com/journalsearch.php?q=21100920033&tip=sid&clean=0
Link Impact Factor :
https://link.springer.com/journal/42461

Overview

Mining, Metallurgy & Exploration is SME's journal covering topics related to mining, mineral and metallurgical processing, and geology and exploration.

- Flagship journal of the Society for Mining, Metallurgy & Exploration (SME).
- Started in 1984 as Minerals & Metallurgical Processing.
- Publishes original research papers, review articles and other communications on matters pertinent to the mining and minerals community.

Executive Editor
Ronel Kappes

Journal Impact Factor
1.5 (2023)

5-year Journal Impact Factor
1.8 (2023)

Submission to first decision (median)
28 days

Downloads
168,663 (2023)

Full artikel

Link artikel :
https://link.springer.com/article/10.1007/s42461-024-00993-5

Mining, Metallurgy & Exploration
https://doi.org/10.1007/s42461-024-00993-5

Integrating Mathews Stability Chart into the Stope Layout Determination Algorithm

Danu Putra[1,3] · Tri Karian[2] · Budi Sulistianto[2] · Mohammad Nur Heriawan[2]

Received: 9 January 2024 / Accepted: 24 April 2024

Abstract
Stope layout optimization is an important feature of underground mining that maximizes the economic value of the project while taking mining limits into account. The large number of parameters and constraints makes it difficult to obtain the optimum condition. Several algorithms have been created to address these problems using a variety of methods. However, the circulating method has not explicitly included stope dimension stability analysis, resulting in a solution that is not stability-proven, which can result in a suboptimal solution. This study integrates the Mathews stability graph into the stope optimization algorithm so that the optimized stope layout considers stability conditions directly through an assessment of the available geomechanical data within the block model. The proposed algorithm is validated through a case study of a synthetic block model created by considering variations in grade and the geomechanical conditions of the rock. Furthermore, several scenarios are created to compare the performance of the algorithm that applies variations in stope sizes with the common case study of stope sizes that remain fixed. A more detailed assessment is also conducted on each final stope layout wall to ensure the successful application of stability analysis in the proposed algorithm through back analysis on the Mathews stability graph. The optimization results show that all walls in the final stope layout fall into the stable condition. Also, the proposed algorithm is also capable of maintaining the project's economic value. Ultimately, the proposed algorithm can be deemed applicable and suitable for use in the initial stages of mining as a comprehensive assessment of the optimal stope layout, taking into account the stability conditions of the stope.

Keywords Stope optimization · Heuristic algorithm · Mathews Stability Chart · Stope layout · Underground mine

1 Introduction

Underground stope stability analysis methods have been widely developed using various techniques such as empirical [1], analytical [2, 3], and numerical [4, 5] in line with the increasing complexity of rock conditions with deeper mining. The increasing complexity of underground mines creates challenges regarding stope design. Poorer rock conditions result in smaller stopes, which then limit reserve, while better rock conditions tend to accommodate bigger stope dimensions [6]. To accommodate the complexity and further simplify the stability analysis, Critical Span Graphs [7] and Mathews Stability Chart [8–10] are two of the empirical approaches that are still widely used as industry standards. These approaches could help engineers determine the stability of stope designs faster, thus making the generation of specific stope designs in certain geomechanical conditions possible. While varying stope dimensions to their specific geomechanical properties could have significant impacts on mine reserves, thus creating more value in mine projects, stope design is often limited in a conservative way, such as when poorer geomechanical data is chosen as the basis for the stope dimension. Furthermore, research integrating stability topics with stope optimization is still limited while such studies are imperative [11].

✉ Tri Karian
tri_karian@itb.ac.id

1 Graduate Program of Mining Engineering, Faculty of Mining and Petroleum Engineering, Institut Teknologi Bandung, Jawa Barat, Bandung 40132, Indonesia

2 Department of Mining Engineering, Faculty of Mining and Petroleum Engineering, Institut Teknologi Bandung, Jawa Barat, Bandung 40132, Indonesia

3 Mining Engineering Department, Faculty of Earth and Energy Technology, Universitas Trisakti, Jakarta Barat, Jakarta, Indonesia

Many stope optimization algorithms have been developed to assist engineers in solving optimization problems [12–14]. Various optimization techniques, such as stochastic [15–17], exact algorithms, and heuristic algorithms [18–20], have been used to ensure that the stope optimization results in maximum NPV with stope dimensions as constraints. The exact algorithm is formed from a mathematical model, ensuring the best solution is obtained. Some algorithms falling into this category include Branch and Bound [21], Dynamic Programming [22], and Downstream Geostatistical Approaches [23]. Dynamic Programming stope optimization was introduced by Riddle [22] in a block-caving case study, which also has its weaknesses due to limitations in its application to that method. Deraime et al. [23] introduced the downstream geostatistical approach to determine parts of the ore body with the best economics. However, the application of this algorithm is limited to cut-and-fill or sublevel stoping methods. The solutions generated by this algorithm cannot yet be considered optimal as they have not been proven with practical mining designs. Ovanic and Young [21] further developed the Branch and Bound algorithm applied to integer programming. Generally, Integer programming requires considerable resources for problem-solving, making it often unfeasible for large case studies. The integration with the Branch and Bound algorithm allows problems to be broken down into smaller ones, making the problem-solving process more efficient. Nevertheless, the effectiveness of solving problems in large case studies remains a weakness, so this algorithm has not been applied beyond one-dimensional case studies.

Contrary to exact algorithms, heuristic algorithms do not focus on mathematical models; thus, the solutions they generate do not fully achieve the global optimum but are close enough to the global optimum. Some algorithms falling into this category include Octree Division [24], Floating Stope [25], Multiple Pass Floating Stope [26], Maximum Neighborhood [27], Topal and Sens [28], and Sandanayake [29]. The Octree Division algorithm introduced by Cheimanoff et al. [24] is capable of working in three-dimensional case studies where the "optimum" part of the block model is determined based on mining constraints and economics. In practice, this algorithm approaches the optimal condition by producing a 3D stope layout. However, the structure of the algorithm, which allows waste blocks to enter the final stope layout, reduces the economic value of the final stope layout. Hence, the optimal solution has not been achieved yet. The next development in stope algorithms, which is quite applicable and adopted in commercial software, is the Floating Stope by Alford [25]. The approach used is similar to other algorithms in open-pit case studies, such as the Floating Cone. Similar to the Floating Cone, one advantage of this algorithm is its simplicity, where a stope of predetermined dimensions is floated on the block model, and an assessment of the stope is conducted to determine its economic feasibility. However, a weakness of this algorithm lies in not considering the important concept of overlapping stopes. Overlapping stope solutions result in double-counted reserves, leading to increased economic feasibility. Adjustments have to be made to ensure that the mined material truly represents the actual mine and its economic value. The need for manual intervention in this algorithm means that the solution from the Floating Stope algorithm cannot yet be considered optimal. To address this weakness, Cawrse [26] developed the Multiple Pass Floating Stope, providing additional information to engineers and making the assessment of the Floating Stope output easier. However, the main weakness of the overlapping stope concept has not been resolved, causing this algorithm to still be unable to produce an optimal solution. Still based on the principle of the Floating Stope, the Maximum Neighborhood algorithm was developed by Ataee-Pour [27]. A more detailed approach, aggregating blocks into stope shapes and, in the process, eliminating blocks with negative economic value, makes this approach better. However, the solutions generated are highly dependent on the initial location of the optimization iterations, causing this algorithm to not yet produce an optimal solution. Later, the heuristic approach developed by Topal and Sens [28] changes geological blocks into economic blocks of uniform size and then forms stopes of specific dimensions in each block model, assessing the stope attributes to see their feasibility. One breakthrough of this approach is the final output of the stope in three dimensions. The structure of the algorithm that sequentially eliminates sets of stopes is a weakness of this approach, making the optimal stope layout not necessarily achievable. Bai [30] developed a heuristic algorithm applied to the sublevel mining method. The limitation of this approach lies in the mining method's conditions and its application, which can only be applied to small ore bodies. Finally, Sandanayake [29] developed a heuristic algorithm by modifying the Floating Stope, where first, the block economic value (BEV) is determined by calculating all economic and geological components within the block. Then, stopes of specific sizes are floated within the block model, while the economic value of the stope is calculated based on the cumulative BEV values entering the stope. Elimination is then carried out on stopes with negative economic value, while sets are formed on stopes with positive values that do not overlap. The set of stopes with the best economic value is chosen as the best solution. However, calculating BEV at the beginning of optimization is one of the weaknesses of this algorithm because economic parameters are independent of mining scenarios, thus the possibility of hidden positive economic value stopes not being further assessed.

The early stope optimization algorithm presented has a common way to express stable stope dimension. The stope, as a mineable area, is typically simplified into a box-shaped dimension with floating width, length, and height [26, 31, 32]. To address practical requirements, dimensional constraints were implemented to ensure that the optimization outcomes met geotechnical and technical conditions [33, 34]. Dimension considerations in optimization are focused on two approaches: fixed dimensions [29, 31] and variable dimensions [35–38]. Fixed dimensions impose uniform, predefined stope dimensions at the initial optimization stage. This constraint limits the algorithm's flexibility in selecting the best stope due to the predetermined size set by the user at the start of optimization. Meanwhile, variable dimensions were applied by setting the maximum and minimum dimension constraints allowed for the stope layout. By providing maximum and minimum dimension constraints, the optimized stope layout fulfills both geomechanical and operational considerations. However, both approaches require users to determine the generally allowable stope size in each optimization domain. Furthermore, variations in rock conditions are not directly considered in the optimization algorithm.

The use of stability analysis in stope optimization algorithm is still limited, used separately from optimization steps, where the most pessimistic geomechanical data is usually used as the basis for determining mining design in a wider area. Limited geomechanical data provides a large amount of uncertainty and eliminates economic potential, as some areas may have marginal value when mined with different stope dimensions. The latest study that adopted stability analysis in optimization algorithms was conducted by Esmaeili et al. [39] by applying stability analysis to the Caving Graph [40] as mining constraints combined with a network flow algorithm. The algorithm was successfully applied to the sublevel caving mining method with limited block numbers. As stope stability analysis methods are widely available, the potential of integrating stability analysis with currently available optimization algorithms is significant. The advantage of this methodology lies in the ability of the algorithm to read and analyze geomechanical data that is already quantitatively available to create stope dimension recommendations. This study aims to integrate Mathews stability analysis [41] into a mining optimization algorithm [32].

2 Proposed Algorithm

Stope designs that represent variations of rock conditions are needed to maximize the project values. In this study, the stope optimization algorithm [31] was modified by adding a stage of stope dimension recommendation based on the Mathews stability graph [41], making the overall algorithm stages as shown in Fig. 1. The approach was carried out by calculating the stability number (N) based on the geomechanical parameters available in the block model, which include *factor A*, *factor B*, *factor C*, and *Q′ value*. *N numbers* are generated throughout iteration based on the available stopes walls that are constrained within the ore body. Further, the maximum allowable hydraulic radius is determined to limit the maximum stope dimension in each block location in the block model. Optimization was then carried out on a similar basis, but with the addition of the geomechanical constraint that was newly proposed.

In this study, the application of the proposed algorithm was limited to the open-stope or sublevel method for metal mines, as the Mathews Stability Chart suggested. Further, consideration of dip angle, thickness, fault, and aquifer of the ore body was considered in the parameters utilized in the Mathews Stability Chart that were already presented in the block model in the form of *factor A*, *B*, *C*, and *Q′* value, while stope wall orientation was limited to vertical as the base of the algorithm was limited to [31].

As for the mathematical models become very complex, Table 1 summarizes the notations, parameters, and decision variables that were used for the subsequent sections.

2.1 Objective Function

The objective function of this study is to maximize the stope economic value by accumulating the block economic value inside the optimum stopes. This was done by utilizing Eq. (1). In order to determine the stopes economic value, two main parameters were used: the geological parameter, including metal grade, and the economic parameter, including metal price and cost components. The block value is calculated in some sequences. First, block tonnage was determined by block lengths and rock density via Eq. (2). After the tonnage values of the blocks are known, the economic value of the block is calculated using Eq. (3) by applying economic parameters such as commodity price, mining cost, processing cost, and selling cost.

$$MAX \sum v_r \times tags \tag{1}$$

$$tr = Ho \times Lo \times Wo \times do \tag{2}$$

$$v_r = \left[\left(p - r_r\right) \times g_r \times y - \left(e_r + c_r\right)\right] \times t_r \tag{3}$$

2.2 Stope Height Constraint

The stope height constraint limits the maximum optimized stope height by ensuring that the cumulative height of mining blocks on the z-axis ($nzs_{i,j,k}$) does not exceed the allowable stope height. Stope height is determined by considering

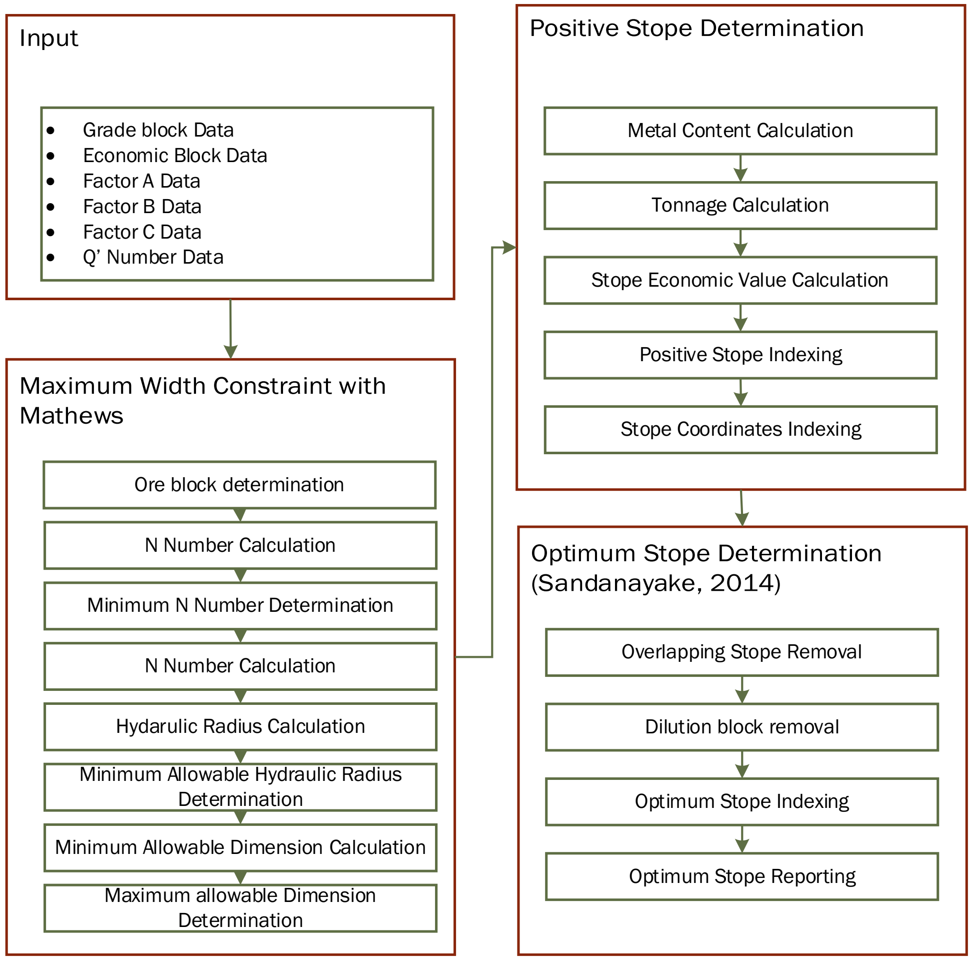

Fig. 1 General algorithm steps

the mining method that is applied in the area and set by the user. Allowing one axis to be fixed decreases the complexity of the algorithm as it will only optimize the stope length and span. However, full consideration needs to be given by the user, as the stope height will also dictate the mining level. A shorter stope will generate many levels and further impact the need for mine access while also creating the opportunity to do selective mining. On the contrary, a higher stope will generate fewer levels, but the production rate could be higher, further impacting the production cost. This condition is displayed in Fig. 2 where the stope's origin, positioned at the lowest elevation of the block model (marked by the green-colored box), is the determining block for the stope's height constraint ($nzs_{i,j,k}$), which also defines the number and location of levels. Nevertheless, the final layout will be driven by the rock conditions, as this constraint only enforces one of the three axes.

In the proposed algorithm, the stope shape is controlled via block quantity relative to its axis. Thus, conversion from allowable stope height to allowable mining block is needed. Equation (4) implies that the maximum stope height is converted by dividing the maximum height by the block height. The calculation was possible because of the regularity of the block size.

$$nzs_{i,j,k} = Hmax/Ho \tag{4}$$

2.3 Maximum and Minimum Width Constraint

The maximum and minimum constraints limit the stope size during the optimization process, ensuring that the optimal stope meets operational and geomechanical criteria. The dimensions of mining equipment are considered the minimum operational width defined by the user ($Wmins$). The stope's width should accommodate the equipment size operating in that area. The use of mechanical equipment tends to require a larger minimum width for the stope compared to traditional mining. In some cases within narrow veins, the equipment width may conflict with the vein width, necessitating a wider stope to compensate for the mechanized mining activities in that location, further impacting the increase in planned dilution, thus reducing the economic feasibility of the stope.

Table 1 List of notations for the mathematical models and methodology

Symbol	Descriptions
Notations	
I	Index position of *x*
J	Index position of *y*
K	Index position of *z*
Parameters	
Ar	Factors A Mathews stability graphs in block
Br	Factors B Mathews stability graphs in block
Cr	Factors C Mathews stability graphs in block
Dr	Rock density
gr	Metal grade in block
gs	Metal grade in stope
Hmax	Maximum stope height
Ho	Block height
HR1r	Hydraulic radius on the 1-th wall of the stope
HR2r	Hydraulic radius on the 2-th wall of the stope
HR3r	Hydraulic radius on the 3-th wall of the stope
HR4r	Hydraulic radius on the 4-th wall of the stope
Lmaxs	Maximum length of stope determined by user
Lmins	Minimum length of stope determined by user
Lo	Block length
mr	Metal weight in block
ms	Metal weight in stope
N1r	*N number* on the 1-th wall of the stope
N2r	*N number* on the 2-th wall of the stope
N3r	*N number* on the 3-th wall of the stope
N4r	*N number* on the 4-th wall of the stope
ni	Number of blocks in *x*-direction
nj	Number of blocks in *y*-direction
nk	Number of blocks in *z*-direction
nxs	N-blocks towards *x* are allowed on the stope
nys	N-blocks towards *y* are allowed on the stope
nzs	N-blocks towards *z* are allowed on the stope
Qr	*Q′* value Q-system in block
tr	Ore tonnage in block
ts	Ore tonnage in stope
vs	Stope economic value
Wo	Block width
Wmins	Minimum width of stope determined by user
Wmaxs	Maximum width of stope determined by the user
Decision variables	
tagr	Tag for ore block
Tags	Tag for ore block in stopes
Ys	Positive stope tag database
Fs	Optimum stope tag database

Differing from the minimum width (*Wmins*), the minimum stope length (*Lmins*) is typically determined based on the length of the stope advancement, where its width is no smaller than the minimum stope advancement length. This constraint ensures that no stope design is created smaller than the stope advance length.

A significant factor affecting the maximum stope width and length (*Wmaxs* and *Lmaxs*) is geomechanics. Solid rock, limited water presence, and favorable stress conditions are indicators of favorable rock conditions where stope sizes can generally be larger to meet production needs. Furthermore, in the design aspect, the orientation of the structure and stope walls can be a determining factor for stability/safety in stope design. Mathews [42] proposed an empirical approach applicable to open stopes or sublevel stoping, where the hydraulic radius and stability number (N') are used as indicators for the maximum stable stope dimensions. The application and integration of the geomechanical constraint model into the stope dimension constraints are explained in more detail in Section 4.

Geomechanical constraints are established by ensuring that the stopes have dimensions smaller than the allowed hydraulic radius at the location where the stopes will be formed. Meanwhile, operational constraints ensure that the dimensions of the stopes are larger than the minimum allowed dimensions at a block model location. Both of these constraints are combined in a unified constraint that regulates the maximum and minimum dimensions along the *x*-axis ($nxs_{i,j,k}$), *y*-axis ($nys_{i,j,k}$), and *z*-axis ($nzs_{i,j,k}$). The stope size is limited by Eq. (5) to (6), which add up the indices of the mined blocks (*tags*) in the stope layout and compare them to the stope size limits. Equations (5), (6), and (7), respectively, operate on the *x*-axis, *y*-axis, and *z*-axis.

$$nxs_{i,j,k} \geq \sum_{i=1}^{I} \sum_{j=1}^{j} \sum_{k=1}^{k} tags \forall \mathrm{i} \in \{1 \ldots \mathrm{I}\}, \mathrm{j} \in \{1 \ldots \mathrm{J}\}, \mathrm{k} \in \{1 \ldots \mathrm{K}\} \tag{5}$$

$$nys_{i,j,k} \geq \sum_{i=1}^{i} \sum_{j=1}^{J} \sum_{k=1}^{k} tags \forall \mathrm{i} \in \{1 \ldots \mathrm{I}\}, \mathrm{j} \in \{1 \ldots \mathrm{J}\}, \mathrm{k} \in \{1 \ldots \mathrm{K}\} \tag{6}$$

$$nzs_{i,j,k} \geq \sum_{i=1}^{i} \sum_{j=1}^{j} \sum_{k=1}^{K} tags \forall \mathrm{i} \in \{1 \ldots \mathrm{I}\}, \mathrm{j} \in \{1 \ldots \mathrm{J}\}, \mathrm{k} \in \{1 \ldots \mathrm{K}\} \tag{7}$$

The application of these equations serves as a constraint in the stope optimization phase, as depicted in Fig. 3. The green-colored blocks depict the block origin's position where the stope dimension constraints are applied, while the dashed red lines represent the boundary of the stope layout's location with the application of stope dimension constraints. With the integrated application of geomechanical considerations in the stope dimension constraint at each stope location, the stope dimensions can be deemed representative as they meet the rock conditions.

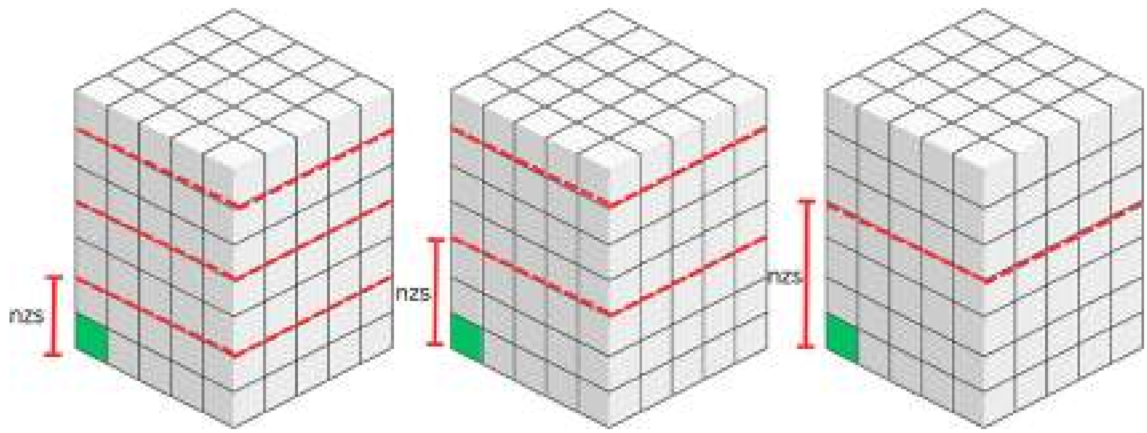

Fig. 2 Stope height constraint

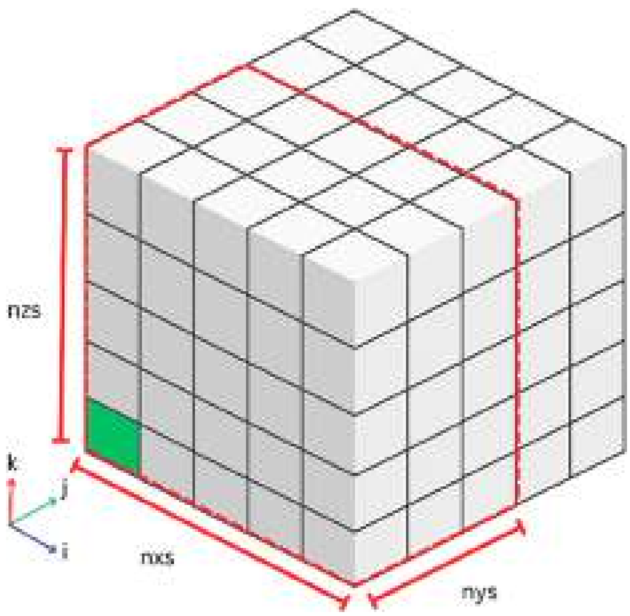

Fig. 3 Stope dimension constraint

2.4 Stope Overlapping Constraint

"Overlapping stopes" is a condition where the optimized stope layouts intersect with each other [33]. This condition arises due to the formation of another optimal stope shape in a nearby location. Overlapping stope results in repeated calculations of volume and tonnage, which then raises the value of the mined material and leads to an overly optimistic assessment of the project's feasibility. Figure 4 depicts an illustration of overlapping stopes where the red-colored

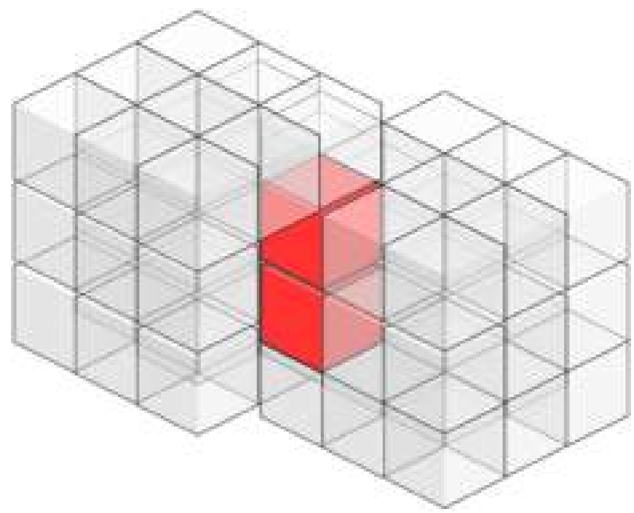

Fig. 4 Overlapping stopes

blocks represent the area where both stopes intersect. In this case, the material attributes within the red blocks will be counted twice, potentially resulting in inaccurate mined material and economic calculations for both stopes.

In this study, the overlap constraint is applied by utilizing the mined block index (*tags*) assigned to each block falling within a stope. The stope layout is deemed feasible when, during stope determination, all blocks within that stope have a mined block index (*tags*) equal to 0. This constraint application ensures that no stope can form in that location if even a single block has a mined block index (*tags*) equal to one. Equation (8) shows the mathematical form of the stope overlap constraint, where $tags_{i,j,k}$ is the mined block indexes.

$$fu1_{i,j,k} = \begin{cases} 0 if tags_{i=1,j=1,k=1}^{i+nxs_{i,j,k},j+nyx_{i,j,k},k+nzs_{i,j,k}} = 1 \\ 1 otherwise \end{cases} \forall \mathrm{i} \in \{1 \ldots \mathrm{I}\}, \mathrm{j} \in \{1 \ldots \mathrm{J}\}, \mathrm{k} \in \{1 \ldots \mathrm{K}\} \quad (8)$$

3 Maximum Width and Span by Mathews Stability Chart

3.1 Mathews Stability Chart

Mathews [42] introduced a stability graph based on 26 cases collected from open-stope underground mining. This data was later supplemented and recalibrated by Potvin [43], which became widely used in the industry as the basis for mine planning that considers rock geomechanics conditions. The stability graph represents a plot of the stability number (N') against the shape factor (S) or also known as the hydraulic radius (HR). The calculation of N' is done by considering Rock Quality Designation *(RQD)*, joint set number (J_n), joint roughness number (J_r), joint alteration number (J_a), stress factor (A), joint orientation factor (B), and gravity factor (C) through Eq. (9). Meanwhile, HR is generally the ratio between the area and the perimeter, which is determined based on the length (L) and width (W) of the stope wall, as shown in Eq. (10). Both of these variable results are plotted on the stability graph to determine the stability condition of the wall through three zones depicted on the graph: stable, unstable, and cave, as seen in Fig. 5.

$$N' = \left(\frac{RQD}{J_n}\right) \times \left(\frac{J_r}{J_a}\right) \times A \times B \times C \quad (9)$$

$$HR = \frac{W \times L}{2 \times (W \times L)} \quad (10)$$

This study employs the stability graph developed by Potvin [43] and Nickson [44] as a stability analysis tool within

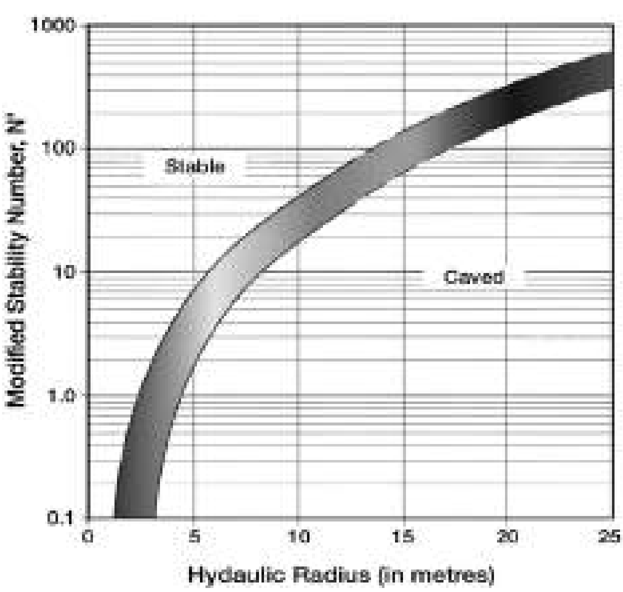

Fig. 5 Potvin-modified Mathews stability graphs [43]

the optimization algorithm. Equation (11) represents the boundary between the stable and unstable areas on the stability graph which was statistically calculated by Nickson [44] based on 175 case studies of stope stability in Potvin [43]. The stope wall dimensions allowed fall within the area above this boundary line. Through the use of this stability graph, it is also assumed that the stopes used in this algorithm are unsupported.

$$HR = 10^{(0.573+0.338\log N')} \quad (11)$$

3.2 Mathews Stability Chart Application in Stope Dimensional Constraint

In this study, improvements to the existing stope optimization algorithm were made by incorporating stability analysis using Mathews Stability Chart into the algorithm as dimensional constraints. Thus, the proposed algorithm has the ability to directly address rock conditions. This was done by assessing the Mathews attribute data provided in the block model. The analysis is conducted at block locations by iterating steps as follows:

1. Assessing the maximum of each stope wall domain by looking for the ore domain.
2. Calculate the *N stability number* based on Q' value*, factor A*, *factor B*, and *factor C* within the wall domain.
3. Determine the stable condition for the wall domain by correlating the hydraulic radius and the *N stability number*.
4. Assessing a smaller domain until a stable condition is met
5. Determine the allowable stope wall dimensions by choosing the lowest hydraulic conditions between each wall.

The algorithm steps are handled by several equations, as follows: Eqs. (12) and (13) are used for the first step, to determine which part of the rock is the ore body, so that subsequent iterations of the equation will be limited to the controlled by the *i*, *j*, and *k* indices of the block. The difference between the two equations lies in the orientation in which each equation is applied. Equation (12) is utilized on the stope wall oriented towards the east, while Eq. (13) is applied on the stope wall oriented towards the north. The calculation of the *N stability number* in the second step is performed by utilizing Eqs. (14) to (17). Each of the equations represents the different calculations performed for the four walls. As seen in the equations, all four equations have different block location indices, representing calculations for block data in different domains of the stope walls. The *N stability number* for each of the stope wall domains is then used to calculate the allowable *hydraulic* *radius* for the corresponding stope wall via Eqs. (18) to (21). Each of the *hydraulic radius* equations corresponds to the wall where it belongs, as the indices specifically emphasize where the calculation is performed.

$$nxs_{i,j,k} = \sum_{i=1}^{Wmax/Wo} \sum_{j=1}^{j} \sum_{k=1}^{k} tagr \forall \mathrm{i} \in \{1 \dots \mathrm{I}\}, \mathrm{j} \in \{1 \dots \mathrm{J}\}, \mathrm{k} \in \{1 \dots \mathrm{K}\} \quad (12)$$

$$nys_{i,j,k} = \sum_{i=1}^{i} \sum_{j=1}^{Lmax/Lo} \sum_{k=1}^{k} tagr \forall \mathrm{i} \in \{1 \dots \mathrm{I}\}, \mathrm{j} \in \{1 \dots \mathrm{J}\}, \mathrm{k} \in \{1 \dots \mathrm{K}\} \quad (13)$$

$$N1r_{i,j,k} = MINNr_{i=1,j=1,k=1}^{i,j+\frac{Lmax}{Lo},nzs} \forall \mathrm{i} \in \{1 \dots \mathrm{I}\}, \mathrm{j} \in \{1 \dots \mathrm{J}\}, \mathrm{k} \in \{1 \dots \mathrm{K}\} \quad (14)$$

$$N2r_{i,j,k} = MINNr_{i=i+(\frac{Wmax}{Wo}),j=1,k=1}^{i+\frac{Wmax}{Wo},j+\frac{Lmax}{Lo},nzs} \forall \mathrm{i} \in \{1 \dots \mathrm{I}\}, \mathrm{j} \in \{1 \dots \mathrm{J}\}, \mathrm{k} \in \{1 \dots \mathrm{K}\} \quad (15)$$

$$N3r_{i,j,k} = MINNr_{i=1,j=1,k=1}^{i+\frac{Wmax}{Wo},j,nzs} \forall \mathrm{i} \in \{1 \dots \mathrm{I}\}, \mathrm{j} \in \{1 \dots \mathrm{J}\}, \mathrm{k} \in \{1 \dots \mathrm{K}\} \quad (16)$$

$$N4r_{i,j,k} = MINNr_{i=1,j=1,k=1}^{i+\frac{Wmax}{Wo},j+\frac{Lmax}{Lo},nzs} \forall \mathrm{i} \in \{1 \dots \mathrm{I}\}, \mathrm{j} \in \{1 \dots \mathrm{J}\}, \mathrm{k} \in \{1 \dots \mathrm{K}\} \quad (17)$$

$$HR1r_{i,j,k} = 10^{(0.573+0.388\times\log(\mathrm{N1r}_{i,j,k}))} \forall \mathrm{i} \in \{1 \dots \mathrm{I}\}, \mathrm{j} \in \{1 \dots \mathrm{J}\}, \mathrm{k} \in \{1 \dots \mathrm{K}\} \quad (18)$$

$$HR2r_{i,j,k} = 10^{(0.573+0.388\times\log(\mathrm{N2r}_{i,j,k}))} \forall \mathrm{i} \in \{1 \dots \mathrm{I}\}, \mathrm{j} \in \{1 \dots \mathrm{J}\}, \mathrm{k} \in \{1 \dots \mathrm{K}\} \quad (19)$$

$$HR3r_{i,j,k} = 10^{(0.573+0.388\times\log(\mathrm{N3r}_{i,j,k}))} \forall \mathrm{i} \in \{1 \dots \mathrm{I}\}, \mathrm{j} \in \{1 \dots \mathrm{J}\}, \mathrm{k} \in \{1 \dots \mathrm{K}\} \quad (20)$$

$$HR4r_{i,j,k} = 10^{(0.573+0.388\times\log(\mathrm{N4r}_{i,j,k}))} \forall \mathrm{i} \in \{1 \dots \mathrm{I}\}, \mathrm{j} \in \{1 \dots \mathrm{J}\}, \mathrm{k} \in \{1 \dots \mathrm{K}\} \quad (21)$$

The selection of the lowest hydraulic radius is then performed on opposing walls to ensure that the lowest value to be used is indicated by Eqs. (22) and (23). The allowable length for stope walls is then determined based on the *hydraulic radius* of the corresponding wall through Eqs. (24) and (25). In the last stage, Eqs. (26) and (27) are making sure that the allowable length for the stope wall has already met operational constraints.

$$HR1r_{i,j,k} = \begin{cases} HR1r_{i,j,k} if HR1r_{i,j,k} < HR2r_{i,j,k} \\ HR2r_{i,j,k} otherwise \end{cases} \forall \mathrm{i} \in \{1 \dots \mathrm{I}\}, \mathrm{j} \in \{1 \dots \mathrm{J}\}, \mathrm{k} \in \{1 \dots \mathrm{K}\} \quad (22)$$

$$HR3r_{i,j,k} = \begin{cases} HR1r_{i,j,k} if HR3r_{i,j,k} < HR4r_{i,j,k} \\ HR4r_{i,j,k} otherwise \end{cases} \forall \mathrm{i} \in \{1 \dots \mathrm{I}\}, \mathrm{j} \in \{1 \dots \mathrm{J}\}, \mathrm{k} \in \{1 \dots \mathrm{K}\} \quad (23)$$

$$nys1_{i,j,k} = \frac{2HR1r_{i,j,k} \times nzs_{i,j,k} \times Ho_{i,j,k}}{(nzs_{i,j,k} \times Ho_{i,j,k}) - 2HR1r_{i,j,k}} \times Lo_{i,j,k} \forall \mathrm{i} \in \{1 \dots \mathrm{I}\}, \mathrm{j} \in \{1 \dots \mathrm{J}\}, \mathrm{k} \in \{1 \dots \mathrm{K}\} \quad (24)$$

$$nxs1_{i,j,k} = \frac{2HR3r_{i,j,k} \times nzs_{i,j,k} \times Ho_{i,j,k}}{(nzs_{i,j,k} \times Ho_{i,j,k}) - 2HR3r_{i,j,k}} \times Lo_{i,j,k} \forall \mathrm{i} \in \{1 \ldots \mathrm{I}\}, \mathrm{j} \in \{1 \ldots \mathrm{J}\}, \mathrm{k} \in \{1 \ldots \mathrm{K}\} \tag{25}$$

$$nxs_{i,j,k} \begin{cases} 0 if\, nxs_{i,j,k} > \frac{Lmins}{Lo} \\ nxs1_{i,j,k} if\, nxs_{i,j,k} > nxs1_{i,j,k} > \frac{Lmins}{Lo} \\ nxs_{i,j,k} otherwise \end{cases} \forall \mathrm{i} \in \{1 \ldots \mathrm{I}\}, \mathrm{j} \in \{1 \ldots \mathrm{J}\}, \mathrm{k} \in \{1 \ldots \mathrm{K}\} \tag{26}$$

$$nys_{i,j,k} \begin{cases} 0 if\, nys_{i,j,k} > \frac{Wmins}{Lo} \\ nys1_{i,j,k} if\, nys_{i,j,k} > nys1_{i,j,k} > \frac{Wmins}{Lo} \\ nys_{i,j,k} otherwise \end{cases} \forall \mathrm{i} \in \{1 \ldots \mathrm{I}\}, \mathrm{j} \in \{1 \ldots \mathrm{J}\}, \mathrm{k} \in \{1 \ldots \mathrm{K}\} \tag{27}$$

4 Optimization

Nhelko A [45] emphasizes the limitations of exact algorithm application in large-scale cases such as stope optimization. Although the resulting solutions may achieve the global optimum, the problem-solving time typically increases exponentially with problem complexity, making this algorithm category infeasible for large-scale cases. Heuristic algorithms are commonly employed solutions for addressing complex problems like stope optimization, ensuring fast problem-solving while still focusing on optimization objectives. This study applies heuristic algorithms in optimization techniques, enabling large-scale cases to serve as a benchmark for algorithm validation. One of the previously developed heuristic algorithms is Sandanayake [29, 31]. Sandanayake [29] introduces a heuristic algorithm for stope optimization with the following general steps:

1. Initialization of all data, parameters, and variables
2. Stope formation through mining block aggregation
3. Update of stope attributes based on mined blocks
4. Extraction of subsets with economic values greater than 0
5. Identification of overlapping stopes
6. Creation of a set containing non-overlapping stopes
7. Calculation of economic value for each non-overlapping stope set
8. Selection of sets and determination of stopes with the highest economic value.

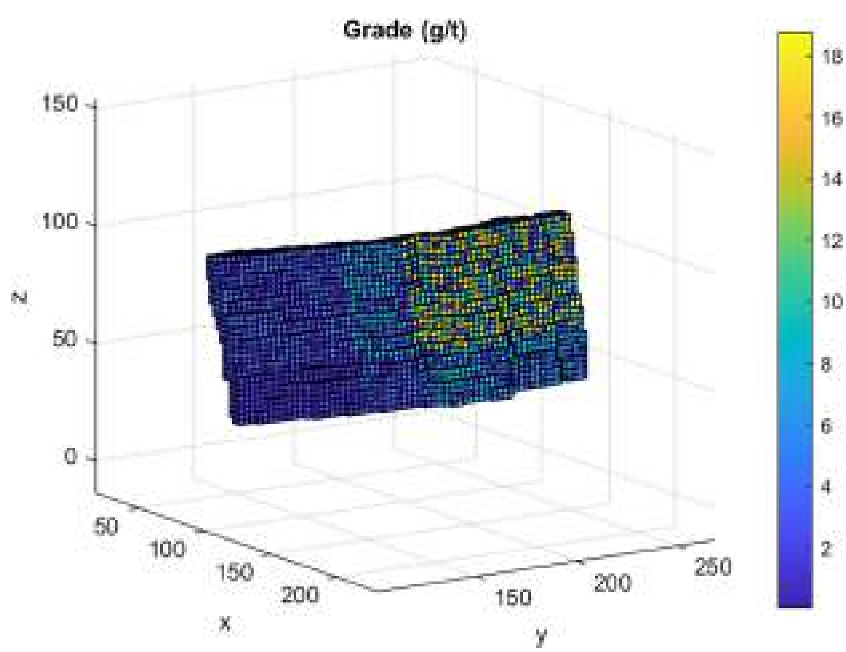

Fig. 6 Block model for Au grade

The algorithm was modified by incorporating Mathews' stability considerations into the stope dimension constraints (*nys*, *nxs*, *nzs*). The varying dimension constraints are held by each block within the block model in line with the geomechanical conditions of that block. Hence, the stope dimensions will vary according to the geomechanical conditions at that location. These constraint applications are implemented in the initial stage of stope creation. The subsequent stage remains relevant, where non-overlapping stopes are created, and ultimately, the stope set with the highest economic value is selected.

5 Case Study

To test the validity of the algorithm proposed in this study, a block model was created by considering several case studies of underground gold mines in Indonesia. Prasetyo et al. [46] modeled a gold vein deposit at one of the mines in Indonesia using the fractal method and compared it to the classical method. In that study, the gold and silver reserves were divided into two zones that were delimited at an elevation of 500 m above sea level. Another study [47] provided an overview of rock mass classes at some underground mines with narrow vein ore types in Indonesia, which were dominated by moderate-to-weak rock. The block model was then created to represent the same conditions.

5.1 The Block Model

Figure 6 explains the uniform dimension block model created from the minimum and maximum ranges of easting, northing, and elevation, respectively, of 100, 100, 35 to 145, 267.5, 102.5. The number of blocks on the *x*, *y*, and *z* axes is 18, 67, and 27, respectively, so the total block model is 32,562. The rock density is set at 2.36 tons/m^3, while the gold grade in the block is divided into six zones, namely upper-high, upper-mid, upper-low, lower-high, lower-mid, and lower-low. The upper and lower zones are separated at an elevation of 60 m above sea level, while the high and mid zones and the mid and low zones are separated at a northing of 210 and 150, respectively. The gold grade in each zone was then created using Eq. (28), where the base grade for each zone (upper-high, upper-mid, upper-low, lower-high, lower-mid, lower-low) is 18.8 g/t, 9.4 g/t, 4.7 g/t, 9.9 g/t, 4.9 g/t, and 2.5 g/t. To better represent the real condition, a random number is introduce to randomize the base Additionally, Table 2 shows the economic parameters used in the block's economic calculation.

The same method is applied to the creation of Q' values in the block model. The Q' model is not divided into upper and lower zones but only into high, mid, and low zones that are delimited by the same northing as previously described. Equation (29) explains how the Q' value is created in the block model, where the Q' base in the high, mid, and low zones is set to 10.1, 1.1, and 2.7, respectively. Sulistianto et al. [48] determined the rock mass class conditions at one of the underground gold mines in Indonesia, which was used as a basis for the value of 0.5 for factors A and B. Factor C is set to 8 because the assessment in this algorithm is only done on the stope walls that have a vertical orientation.

Table 2 Economic parameter

Parameter	Value
Metal price ($/gram)	54.8
Mining cost ($/ton)	35.8
Processing cost ($/ton)	1.6
Refining cost ($/ton)	3.9
Global recovery (%)	80

$$AuGrade\prime = randomnumber \times Augradebase \tag{28}$$

$$Q\prime = randomnumber \times Q\prime base \tag{29}$$

5.2 The Test Methodology

A number of scenarios are used to see the performance of the Mathews analysis in the algorithm that can produce the stope dimension variable in the algorithm. In this validation, three scenarios are used, including the fixed maximum stope dimension, the fixed minimum stope dimension, and the proposed algorithm, which are subsequently referred to as scenarios 1, 2, and 3. The three scenarios were created to explore the optimization potential of stopes with varied shapes due to the variations in rock conditions compared to the commonly practiced optimization based on fixed dimensions. Scenarios 1 and 2 represent optimization with fixed dimensions, while scenario 3 represents stopes with varied. Nevertheless, to enable a comparison between scenarios, the stope height for each scenario is set at 5 m.

In scenario 1, the stope dimension is set according to the maximum dimension allowed based on best geomechanical conditions found in the block model data. The calculations are performed based on the N' value for the best rock condition found in the block model. The largest dimension is determined by calculating the *HR* value for that rock condition. Because the stope height is fixed, the width (l) and length (w) of the stope can be determined. It is known that

Table 3 Validation scenarios

Scenario	Stope dimension ($l \times w \times h$) (m)
Scenario 1	7.5×7.5×5
Scenario 2	5×5×5
Scenario 3	Variable

Table 4 Optimization results

Parameter	Scenario 1	Scenario 2	Scenario 3
Number of stopes	195	711	302
Mined tonnage (ton)	238,777	214,161	165,658
Mined metal (grams)	864,736	949,086	856,880
Mined average grade (g/t)	3.62	4.43	5.17
Economic value ($)	26,283,967	30,640,495	28,700,093

the width and length of the stope based on the rock condition in the block model are 7.5 m. Compared to scenario 1, the minimum stope width and length allowed in scenario 2 is based on operational considerations set at 5 m. This minimum dimension is also applied in scenario 3 as the basis for achieving operational considerations in the optimization phase. The optimization application based on geomechanical considerations is manifested in scenario 3, where the algorithm is given the freedom to determine stope dimensions according to the geological, economic, and geomechanical considerations available in the block model. The scenarios in this case study are seen in Table 3.

To assess the validity of stability analysis application within the stope optimization algorithm, a validation was conducted through back analysis on the final stope walls. Analysis on all four stope walls was carried out by plotting the hydraulic radius (*HR*) of the stope wall against the stability number (*S*). The optimization results can be considered valid if all plots of the stope walls fall within the stable zone. Further details are provided in Section 8.

6 Results

Table 4 shows the results of the optimization in the three scenarios, while the results of the stopes that have been optimized are shown in Fig. 7. From Table 4, it can be seen that the integration of the Mathews stability module into the algorithm

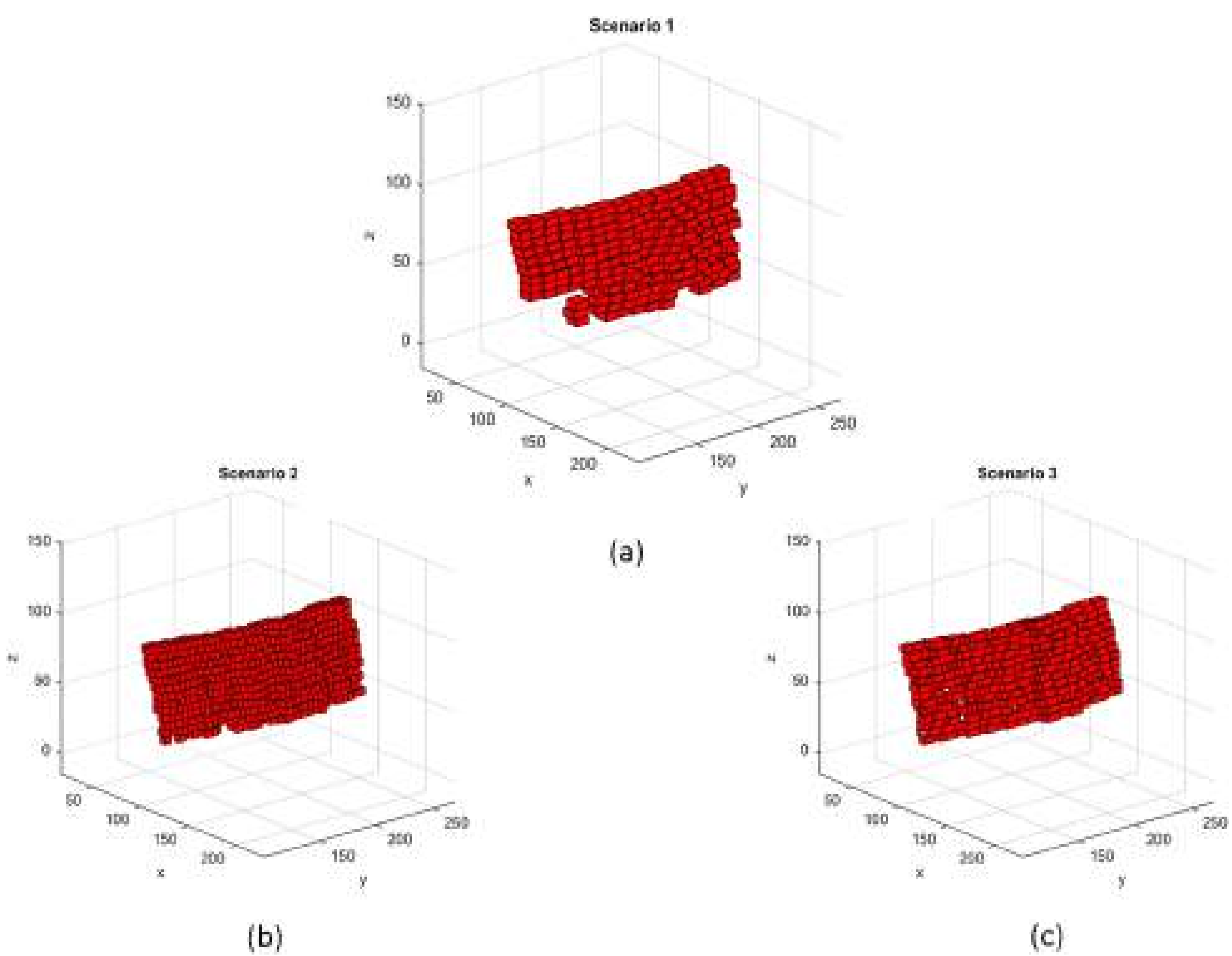

Fig. 7 **a–c** Optimized stopes

in scenario 3 has a level of economy that is competitive with the optimization of the fixed dimension stopes. In general, the varied shape of the stope, following the ore shape, provides an advantage in minimizing mined material waste, as indicated by the highest mined grade among the three scenarios. Furthermore, mining can be considered more efficient. The smaller amount of mined material in scenario 3 indicates that there is less material to be moved for a higher economic value.

In scenario 2, however, the value of the stopes is higher than in scenario 3, which is considered normal for optimization to be carried out on the same cost components in each scenario. As optimization is carried out on the same cost basis across all scenarios, the results will tend towards smaller dimensioned stopes as they can maximize the reserves. In actual case studies, smaller stopes can lead to lower productivity, resulting in relatively smaller economic value due to higher mining costs. The further relationship between the dimensions and the cost of the stopes needs to be established for the algorithm to perform better.

Figure 7 shows the visualization of the optimized stope in all three scenarios. Scenario 1 is unable to maximize the reserves in areas with low grades because the large stope size causes a lot of mined waste material, so the profit from mining ore must compensate for this. This condition is visible in Fig. 7a at low elevations in the southern part, where no stopes are formed in those locations, indicating stopes with negative economic value. In contrast, scenario 2 (Fig. 7b) and scenario 3 (Fig. 7c) showed the opposite results, where the smaller stope dimensions in scenario 2 were able to accommodate ore grade variations better, while the flexibility in dimension selection in scenario 3 had the same effect.

7 Stability Confirmation with Mathews

Validation of stope stability was performed on each final stope wall formed in scenario 3. The stability number (*S*) values for each wall were plotted against the corresponding hydraulic radius (*HR*) values of the stope wall to determine the stability condition of each wall using Mathews' stability graph. Based on the back analysis plots conducted, all of the optimized stope walls have stable conditions, as indicated by the stability points plotted above the stability line in Fig. 3. In the hanging wall and footwall areas, all stope walls can be considered stable, as seen in Fig. 8 (left). The distribution of the plots tends to be vertical, indicating variations in the rock conditions within the block model, while the tight horizontal distribution indicates consistent stope wall areas. A similar pattern is observed in the distribution of plots for the front wall and back wall (Fig. 8 (right)), suggesting a similar condition in those areas. The tight horizontal distribution also indicates minimal variations in the length or width of the formed stopes, which is commonly observed in narrow deposit formations as utilized in this case study. Further, the application of the Mathews stability analysis to the optimization algorithm was deemed successful, as indicated by the good stope economic values and stable conditions at each stope wall.

8 Conclusions

One of the significant challenges in underground mine planning is determining the stope layout, which involves the location, wall area, and stope size. The stope layout

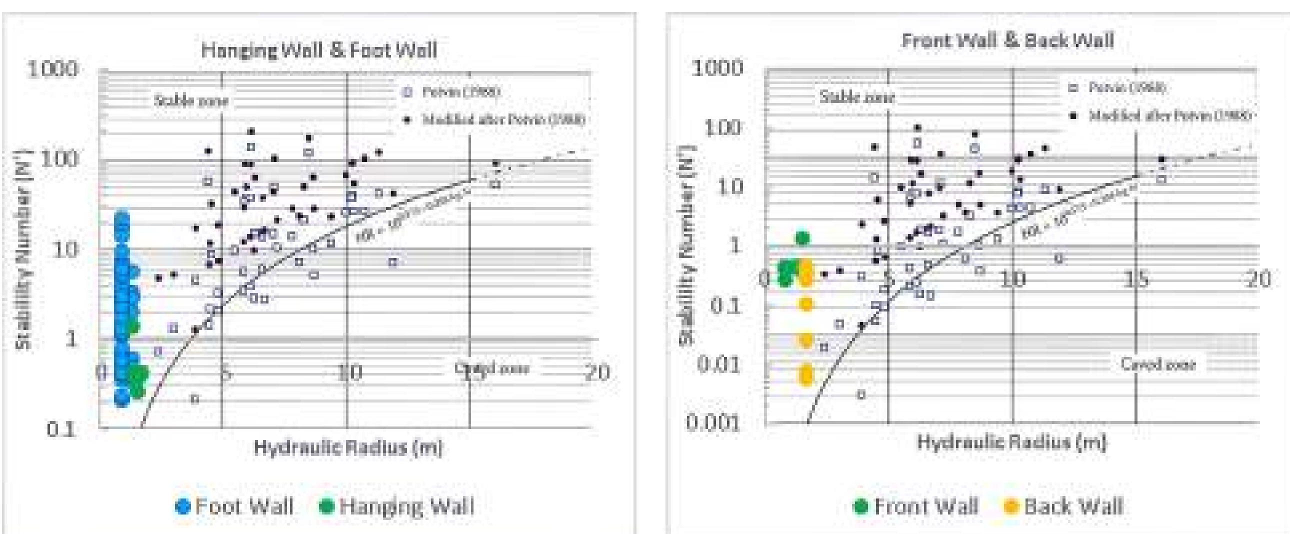

Fig. 8 Stability analysis for optimized stope wall

dictates the amount of material extracted, the metal content, and grade of minerals extracted, ultimately determining the aggregate economic value of all extracted stopes. Addressing this challenge has been largely done through the development of optimization algorithms, enabling mining engineers to assess various stope layouts more efficiently. However, the involvement of numerous parameters renders optimization algorithms susceptible to suboptimal conditions, wherein the stope layout produced by the optimization process may not be the best solution achievable for a given case study. Among the multitude of parameters involved, rock conditions are one of the dominant parameters considered in determining the stope layout. The study's proposed algorithm tried to combine the steps of stope optimization with stability analysis using the Mathews Stability Chart. This was done so that a more complete design could be made, especially since more field data about the geomechanical properties was available.

Integration is suggested by establishing dimensional constraint at the onset of optimization utilizing Mathews stability analysis. This involves incorporating geomechanical data, such as rock mass classification Q', factor A, factor B, and factor C. The outcomes demonstrate the effectiveness of this approach, evident in the optimization outcomes that yield superior economic value compared to employing fixed dimensions. Furthermore, the stability of the optimized stope walls affirms the effectiveness of stability analysis within the optimization algorithm, ensuring the project's financial feasibility. The results of optimization by this algorithm could serve as preliminary guidance for mine planners during the feasibility evaluation phase.

Author Contribution Conceptualization, software, investigation, visualization, writing—review and editing, and project administration: Danu Putra; methodology, validation, formal analysis, and writing—review and editing: Tri Karian; validation, resources, writing—review and editing, supervision, and funding acquisition: Budi Sulistianto; supervision, resources, validation, and writing—review and editing: Mohamad Nur Heriawan.

Funding The authors express great appreciation to Institut Teknologi Bandung through the Riset Unggulan ITB 2022 for funding this study.

Data Availability The data that support the finding of this study are available from the corresponding author upon reasonable request.

Declarations

Competing Interests The authors declare no competing interests.

References

1. Mawdesley C, Trueman R, Whiten WJ (2001) Extending the Mathews stability graph for open–stope design. Min Technol 110:27–39. https://doi.org/10.1179/mnt.2001.110.1.27
2. Lu A, Yin C, Zhang N (2019) Analytic stress solutions for a lined circular tunnel under frictional slip contact conditions. Eur J Mech A Solids 75:10–20. https://doi.org/10.1016/J.EUROMECHSOL.2019.01.008
3. Vitali OPM, Celestino TB, Bobet A (2019) Shallow tunnels misaligned with geostatic principal stress directions: analytical solution and 3d face effects. Tunn Undergr Space Technol 89:268–283. https://doi.org/10.1016/J.TUST.2019.04.006
4. Napa-García GF, Câmara TR, and Navarro Torres VF (2019) Optimization of room-and-pillar dimensions using automated numerical models. Int J Min Sci Technol 29: https://doi.org/10.1016/J.IJMST.2019.02.003.
5. Abdellah WR, Ahmed HM, Hefni MA (2019) Numerical modelling of staged stope extraction in a tabular steeply dipping deposit. Geomech Geoeng 14:41–51. https://doi.org/10.1080/17486025.2018.1508856
6. Mensah T (2023) A binary integer linear programming model for optimizing a binary integer linear programming model for optimizing underground stope layout underground stope layout. https://scholarsmine.mst.edu/masters_theses/8176
7. Lowson AR, Bieniawski ZT (2013) Critical assessment of RMR based tunnel design practices: a practical engineer's approach. SME
8. Kang Z et al (2019) Optimization calculation of stope structure parameters based on Mathews stabilization graph method. J Vibroeng 21:1227–1239
9. Wang D et al (2021) Stope stability assessment by the Mathews-Potvin method: a case-study of open stoping in salt rock mass under conditions of secondary stress field. IOP Publishing. https://doi.org/10.1088/1755-1315/684/1/012011
10. Liu H, Zhao Y, Zhang P, Liu F, Yang T (2021) Stope structure evaluation based on the damage model driven by microseismic data and Mathews stability diagram method in Xiadian gold mine. Geomat Nat Haz Risk 12:1616–1637. https://doi.org/10.1080/19475705.2021.1941308
11. Janiszewski M, Pontow S, Rinne M (2021) Industry survey on the current state of stope design methods in the underground mining sector. Energies (Basel) 15:240. https://doi.org/10.3390/en15010240
12. Nikbin V, Ataee-pour M, Shahriar K, Pourrahimian Y, MirHassani SA (2018) Stope boundary optimization: a mathematical model and efficient heuristics. Resour Policy 62:515–526. https://doi.org/10.1016/J.RESOURPOL.2018.10.007
13. Basiri Z (2018) Stopes layout and production scheduling optimization in sublevel stoping mining. Dissertation, University of Alberta
14. Nelis G, Gamache M, Marcotte D, Bai X (2016) Stope optimization with vertical convexity constraints. Optim Eng 17:813–832. https://doi.org/10.1007/s11081-016-9321-6
15. Wilson B (2020) Heuristic stochastic stope layout optimization. University of Alberta, Thesis
16. Furtado e Faria M, Dimitrakopoulos R, and Lopes Pinto CL (2022) Integrated stochastic optimization of stope design and long-term underground mine production scheduling. Resources Policy 78: https://doi.org/10.1016/j.resourpol.2022.102918.
17. Furtado e Faria MA, Dimitrakopoulos R, Pinto C (2022) Stochastic stope design optimisation under grade uncertainty and dynamic development costs. Int J Min Reclam Environ 36:81–103. https://doi.org/10.1080/17480930.2021.1968707

18. Sari YA, Kumral M (2021) Sublevel stope layout planning through a greedy heuristic approach based on dynamic programming. J Oper Res Soc 72:554–563. https://doi.org/10.1080/01605682.2019.1700179
19. Tolouei K, Moosavi E, Tabrizi AHB, Afzal P, Bazzazi AA (2021) An optimisation approach for uncertainty-based long-term production scheduling in open-pit mines using meta-heuristic algorithms. Int J Min Reclam Environ 35:115–140. https://doi.org/10.1080/17480930.2020.1773119
20. Lamghari A, Dimitrakopoulos R (2020) Hyper-heuristic approaches for strategic mine planning under uncertainty. Comput Oper Res 115:104590. https://doi.org/10.1016/j.cor.2018.11.010
21. Ovanic J, Young DS (1995) Economic optimisation of stope geometry using separable programming with special branch and bound techniques. McGill University
22. Riddle JM (1977) Dynamic programming solution of a block-caving mine layout. 767–780. https://www.onemine.org/documents/a-dynamic-programming-solution-of-a-block-caving-mine-layout Accessed: Jan. 26, 2023
23. Deraisme J, De Fouquet C, Fraisse H (1984) Geostatistical orebody model computer optimization of profits from different underground mining methods. 583–590
24. Cheimanoff NM, Deliac EP, Mallet JL (1989) GEOCAD: an alternative cad and artificial intelligence tool that helps moving from geological resources to mineable reserves. Publ by Soc of Mining Engineers of AIME
25. Alford C (1995) Optimisation in underground mine design.
26. Cawrse I (2001) Multiple pass floating stope process.
27. Ataee-Pour M (2004) Optimisation of stope limits using a heuristic approach. Inst Mining Metall Trans Sect A: Min Technol 113: https://doi.org/10.1179/037178404225004959.
28. Topal E, Sens J (2010) A new algorithm for stope boundary optimization. J Coal Sci Eng 16:113–119. https://doi.org/10.1007/s12404-010-0201-y
29. Sandanayake DSS, Topal E, Ali Asad MW (2015) A heuristic approach to optimal design of an underground mine stope layout. Appl Soft Comput 30:595–603. https://doi.org/10.1016/J.ASOC.2015.01.060
30. Bai X, Marcotte D, Simon R (2013) Underground stope optimization with network flow method. Comput Geosci 52:361–371. https://doi.org/10.1016/j.cageo.2012.10.019
31. Sandanayake DSS, Topal E, Asad MWA (2015) Designing an optimal stope layout for underground mining based on a heuristic algorithm. Int J Min Sci Technol 25:767–772. https://doi.org/10.1016/j.ijmst.2015.07.011
32. Sandanayake DSS (2014) Stope boundary optimisation in underground mining based on a heuristic approach. Dissertation, Curtin University
33. Sari YA, Kumral M (2019) A planning approach for polymetallic mines using a sublevel stoping technique with pillars and ultimate stope limits. Eng Optim 52:932–944. https://doi.org/10.1080/0305215X.2019.1624739
34. Sari YA, Kumral M (2021) Clustering-based iterative approach to stope layout optimization for sublevel stoping. J South Afr Inst Min Metall 121:97–106. https://doi.org/10.17159/2411-9717/1237/2021
35. Kumral M, Sari YA (2020) Underground mine planning for stope-based methods. AIP Publishing LLC 10(1063/5):0006787
36. Villalba Matamoros ME, Kumral M (2017) Heuristic stope layout optimisation accounting for variable stope dimensions and dilution management. Int J Min Miner Eng 8:1–18. https://doi.org/10.1504/IJMME.2017.082680
37. Hou J, Xu C, Dowd PA, Li G (2019) Integrated optimisation of stope boundary and access layout for underground mining operations. Min Technol 128:193–205. https://doi.org/10.1080/25726668.2019.1603920
38. V Nikbin E Mardaneh M Waqar A Asad E Topal 2021 Pattern search method for accelerating stope boundary optimization problem in underground mining operations https://doi.org/10.1080/0305215X.2021.1932869
39. Esmaeili A, Hamidi JK, Mousavi A (2023) Determination of sublevel stoping layout using a network flow algorithm and the MRMR classification system. Resour Policy 80:103265. https://doi.org/10.1016/J.RESOURPOL.2022.103265
40. Laubscher DH (1990) A geomechanics classification system for the rating of rock mass in mine design. J South Afr Inst Min Metall 90:257–273
41. Potvin Y, Hadjigeorgiou J (2001) The stability graph method. Underground Mining Methods 66:513–520
42. Mathews, K. E. Hoek, D. C. Wyllie, and S. B. V. Stewart (1980) Prediction of stable excavation spans for mining at depths below 1000 metres in hard rock. https://www.scirp.org/(S(i43dyn45teexjx455qlt3d2q))/reference/ReferencesPapers.aspx?ReferenceID=1053122 Accessed: Mar. 02, 2020
43. Potvin Y (1988) Empirical open stope design in Canada. University of British Columbia
44. Nickson SD (1992) Cable support guidelines for hard rock mine operations. University of British Columbia
45. Nhleko A, Tholana T, Neingo P (2018) A review of underground stope boundary optimization algorithms. Resour Policy 56:59–69. https://doi.org/10.1016/J.RESOURPOL.2017.12.004
46. Prasetyo E (2010) Fractal model and classical block model in ore reserve estimation: a comparison. Riset Geologi Dan Pertambangan 20:119–130
47. Purwanto SH, Sasaoka T, Wattimena RK, Matsui K, Matsui K (2013) Influence of stope design on stability of hanging wall decline in Cibaliung underground gold mine. Int J Geosci 04:1–8. https://doi.org/10.4236/ijg.2013.410A001
48. Budi S, Wattimena RK, Ardianto A, Matsui K (2009) Determination of stope geometry in jointed rock mass at Pongkor underground gold mine. Int J JCRM 5:63–68. https://doi.org/10.11187/ijjcrm.5.63

Integration of Stability Factor A, B, and C on Mathews Stability Graph

by Danu Putra FTKE

Submission date: 13-Feb-2025 11:55PM (UTC+0700)
Submission ID: 2587653960
File name: 557acc11-c4bd-4648-abac-f99f01111f05.pdf (2.34M)
Word count: 8676
Character count: 45465

Mining, Metallurgy & Exploration
https://doi.org/10.1007/s42461-024-00993-5

Integrating Mathews Stability Chart into the Stope Layout Determination Algorithm

Danu Putra[1,3] · Tri Karian[2] · Budi Sulistianto[2] · Mohammad Nur Heriawan[2]

Received: 1 January 2024 / Accepted: 24 April 2024

Abstract
Stope layout optimization is an important phase of underground mining that maximizes the economic value of the project while taking mining limits into account. The large number of parameters and constraints makes it difficult to obtain the optimum condition. Several algorithms have been created to address these problems using a variety of methods. However, the circulating method has not explicitly included stope dimension stability analysis, resulting in a solution that is not stability-proven, which can result in a suboptimal solution. This study integrates the Mathews stability graph into the stope optimization algorithm so that the optimized stope layout considers stability conditions directly through an assessment of the available geomechanical data within the block model. The proposed algorithm is validated through a case study of a synthetic block model created by considering variations in grade and the geomechanical conditions of the rock. Furthermore, several scenarios are created to compare the performance of the algorithm that applies variations in stope sizes with the common case study of stope sizes that remain fixed. A more detailed assessment is also conducted on each final stope layout wall to ensure the successful application of stability analysis in the proposed algorithm through back analysis on the Mathews stability graph. The optimization results show that all walls in the final stope layout fall into the stable condition. Also, the proposed algorithm is also capable of maintaining the project's economic value. Ultimately, the proposed algorithm can be deemed applicable and suitable for use in the initial stages of mining as a comprehensive assessment of the optimal stope layout, taking into account the stability conditions of the stope.

Keywords Stope optimization · Heuristic algorithm · Mathews Stability Chart · Stope layout · Underground mine

1 Introduction

Underground stope stability analysis methods have been widely developed using various techniques such as empirical [1], analytical [2, 3], and numerical [4, 5] in line with the increasing complexity of rock conditions with deeper mining. The increasing complexity of underground mines creates challenges regarding stope design. Poorer rock conditions result in smaller stopes, which then limit reserve, while better rock conditions tend to accommodate bigger stope dimensions [6]. To accommodate the complexity and further simplify the stability analysis, Critical Span Graphs [7] and Mathews Stability Chart [8–10] are two of the empirical approaches that are still widely used as industry standards. These approaches could help engineers determine the stability of stope designs faster, thus making the generation of specific stope designs in certain geomechanical conditions possible. While varying stope dimensions to their specific geomechanical properties could have significant impacts on mine reserves, thus creating more value in mine projects, stope design is often limited in a conservative way, such as when poorer geomechanical data is chosen as the basis for the stope dimension. Furthermore, research integrating stability topics with stope optimization is still limited while such studies are imperative [11].

✉ Tri Karian
tri_karian@itb.ac.id

1 Graduate Program of Mining Engineering, Faculty of Mining and Petroleum Engineering, Institut Teknologi Bandung, Jawa Barat, Bandung 40132, Indonesia

2 Department of Mining Engineering, Faculty of Mining and Petroleum Engineering, Institut Teknologi Bandung, Jawa Barat, Bandung 40132, Indonesia

3 Mining Engineering Department, Faculty of Earth and Energy Technology, Universitas Trisakti, Jakarta Barat, Jakarta, Indonesia

Published online: 22 May 2024

Many stope optimization algorithms have been developed to assist engineers in solving optimization problems [12–14]. Various optimization techniques, such as stochastic [15–17], exact algorithms, and heuristic algorithms [18–20], have been used to ensure that the stope optimization results in maximum NPV with stope dimensions as constraints. The exact algorithm is formed from a mathematical model, ensuring the best solution is obtained. Some algorithms falling into this category include Branch and Bound [21], Dynamic Programming [22], and Downstream Geostatistical Approaches [23]. Dynamic Programming stope optimization was introduced by Riddle [22] in a block-caving case study, which also has its weaknesses due to limitations in its application to that method. Deraisme et al. [23] introduced the downstream geostatistical approach to determine parts of the ore body with the best economics. However, the application of this algorithm is limited to cut-and-fill or sublevel stoping methods. The solutions generated by this algorithm cannot yet be considered optimal as they have not been proven with practical mining designs. Ovanic and Young [21] further developed the Branch and Bound algorithm applied to integer programming. Generally, Integer programming requires considerable resources for problem-solving, making it often unfeasible for large case studies. The integration with the Branch and Bound algorithm allows problems to be broken down into smaller ones, making the problem-solving process more efficient. Nevertheless, the effectiveness of solving problems in large case studies remains a weakness, so this algorithm has not been applied beyond one-dimensional case studies.

Contrary to exact algorithms, heuristic algorithms do not focus on mathematical models; thus, the solutions they generate do not fully achieve the global optimum but are close enough to the global optimum. Some algorithms falling into this category include Octree Division [24], Floating Stope [25], Multiple Pass Floating Stope [26], Maximum Neighborhood [27], Topal and Sens [28], and Sandanayake [29]. The Octree Division algorithm introduced by Cheimanoff et al. [24] is capable of working in three-dimensional case studies where the "optimum" part of the block model is determined based on mining constraints and economics. In practice, this algorithm approaches the optimal condition by producing a 3D stope layout. However, the structure of the algorithm, which allows waste blocks to enter the final stope layout, reduces the economic value of the final stope layout. Hence, the optimal solution has not been achieved yet. The next development in stope algorithms, which is quite applicable and adopted in commercial software, is the Floating Stope by Alford [25]. The approach used is similar to other algorithms in open-pit case studies, such as the Floating Cone. Similar to the Floating Cone, one advantage of this algorithm is its simplicity, where a stope of predetermined dimensions is floated on the block model, and an assessment of the stope is conducted to determine its economic feasibility. However, a weakness of this algorithm lies in not considering the important concept of overlapping stopes. Overlapping stope solutions result in double-counted reserves, leading to increased economic feasibility. Adjustments have to be made to ensure that the mined material truly represents the actual mine and its economic value. The need for manual intervention in this algorithm means that the solution from the Floating Stope algorithm cannot yet be considered optimal. To address this weakness, Cawrse [26] developed the Multiple Pass Floating Stope, providing additional information to engineers and making the assessment of the Floating Stope output easier. However, the main weakness of the overlapping stope concept has not been resolved, causing this algorithm to still be unable to produce an optimal solution. Still based on the principle of the Floating Stope, the Maximum Neighborhood algorithm was developed by Ataee-Pour [27]. A more detailed approach, aggregating blocks into stope shapes and, in the process, eliminating blocks with negative economic value, makes this approach better. However, the solutions generated are highly dependent on the initial location of the optimization iterations, causing this algorithm to not yet produce an optimal solution. Later, the heuristic approach developed by Topal and Sens [28] changes geological blocks into economic blocks of uniform size and then forms stopes of specific dimensions in each block model, assessing the stope attributes to see their feasibility. One breakthrough of this approach is the final output of the stope in three dimensions. The structure of the algorithm that sequentially eliminates sets of stopes is a weakness of this approach, making the optimal stope layout not necessarily achievable. Bai [30] developed a heuristic algorithm applied to the sublevel mining method. The limitation of this approach lies in the mining method's conditions and its application, which can only be applied to small ore bodies. Finally, Sandanayake [29] developed a heuristic algorithm by modifying the Floating Stope, where first, the block economic value (BEV) is determined by calculating all economic and geological components within the block. Then, stopes of specific sizes are floated within the block model, while the economic value of the stope is calculated based on the cumulative BEV values entering the stope. Elimination is then carried out on stopes with negative economic value, while sets are formed on stopes with positive values that do not overlap. The set of stopes with the best economic value is chosen as the best solution. However, calculating BEV at the beginning of optimization is one of the weaknesses of this algorithm because economic parameters are independent of mining scenarios, thus the possibility of hidden positive economic value stopes not being further assessed.

The early stope optimization algorithm presented has a common way to express stable stope dimension. The stope, as a mineable area, is typically simplified into a box-shaped dimension with floating width, length, and height [26, 31, 32]. To address practical requirements, dimensional constraints were implemented to ensure that the optimization outcomes met geotechnical and technical conditions [33, 34]. Dimension considerations in optimization are focused on two approaches: fixed dimensions [29, 31] and variable dimensions [35–38]. Fixed dimensions impose uniform, predefined stope dimensions at the initial optimization stage. This constraint limits the algorithm's flexibility in selecting the best stope due to the predetermined size set by the user at the start of optimization. Meanwhile, variable dimensions were applied by setting the maximum and minimum dimension constraints allowed for the stope layout. By providing maximum and minimum dimension constraints, the optimized stope layout fulfills both geomechanical and operational considerations. However, both approaches require users to determine the generally allowable stope size in each optimization domain. Furthermore, variations in rock conditions are not directly considered in the optimization algorithm.

The use of stability analysis in stope optimization algorithm is still limited, used separately from optimization steps, where the most pessimistic geomechanical data is usually used as the basis for determining mining design in a wider area. Limited geomechanical data provides a large amount of uncertainty and eliminates economic potential, as some areas may have marginal value when mined with different stope dimensions. The latest study that adopted stability analysis in optimization algorithms was conducted by Esmaeili et al. [39] by applying stability analysis to the Caving Graph [40] as mining constraints combined with a network flow algorithm. The algorithm was successfully applied to the sublevel caving mining method with limited block numbers. As stope stability analysis methods are widely available, the potential of integrating stability analysis with currently available optimization algorithms is significant. The advantage of this methodology lies in the ability of the algorithm to read and analyze geomechanical data that is already quantitatively available to create stope dimension recommendations. This study aims to integrate Mathews stability analysis [41] into a mining optimization algorithm [32].

2 Proposed Algorithm

Stope designs that represent variations of rock conditions are needed to maximize the project values. In this study, the stope optimization algorithm [31] was modified by adding a stage of stope dimension recommendation based on the Mathews stability graph [41], making the overall algorithm stages as shown in Fig. 1. The approach was carried out by calculating the stability number (*N*) based on the geomechanical parameters available in the block model, which include *factor A*, *factor B*, *factor C*, and *Q'* value. *N numbers* are generated throughout iteration based on the available stopes walls that are constrained within the ore body. Further, the maximum allowable hydraulic radius is determined to limit the maximum stope dimension in each block location in the block model. Optimization was then carried out on a similar basis, but with the addition of the geomechanical constraint that was newly proposed.

In this study, the application of the proposed algorithm was limited to the open-stope or sublevel method for metal mines, as the Mathews Stability Chart suggested. Further, consideration of dip angle, thickness, fault, and aquifer of the ore body was considered in the parameters utilized in the Mathews Stability Chart that were already presented in the block model in the form of *factor A, B, C,* and *Q'* value, while stope wall orientation was limited to vertical as the base of the algorithm was limited to [31].

As for the mathematical models become very complex, Table 1 summarizes the notations, parameters, and decision variables that were used for the subsequent sections.

2.1 Objective Function

The objective function of this study is to maximize the stope economic value by accumulating the block economic value inside the optimum stopes. This was done by utilizing Eq. (1). In order to determine the stopes economic value, two main parameters were used: the geological parameter, including metal grade, and the economic parameter, including metal price and cost components. The block value is calculated in some sequences. First, block tonnage was determined by block lengths and rock density via Eq. (2). After the tonnage values of the blocks are known, the economic value of the block is calculated using Eq. (3) by applying economic parameters such as commodity price, mining cost, processing cost, and selling cost.

$$MAX \sum v_e \times x_{ijk} \tag{1}$$

$$tr = Hn \times Ln \times Wn \times dn \tag{2}$$

$$v_e = \left[(p - r_c) \times g_i \times r - (c_r + c_c) \right] \times t_r \tag{3}$$

2.2 Stope Height Constraint

The stope height constraint limits the maximum optimized stope height by ensuring that the cumulative height of mining blocks on the z-axis ($nz_{i,j,k}$) does not exceed the allowable stope height. Stope height is determined by considering

Fig. 1 General algorithm steps

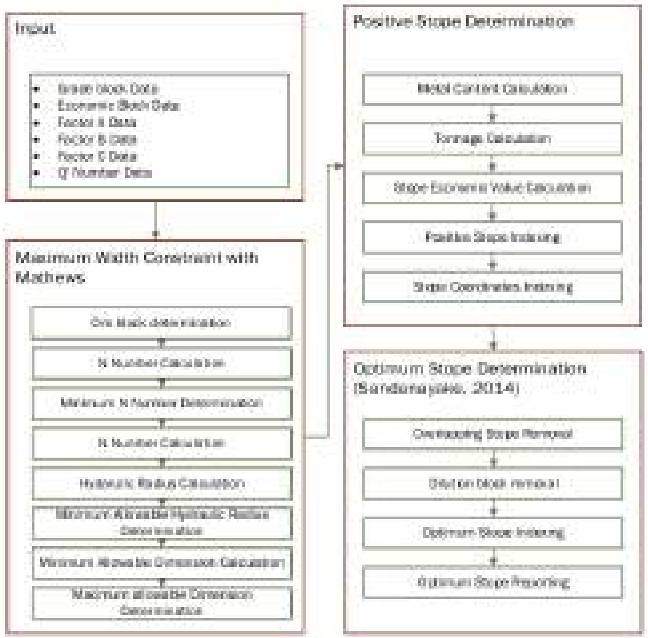

the mining method that is applied in the area and set by the user. Allowing one axis to be fixed decreases the complexity of the algorithm as it will only optimize the stope length and span. However, full consideration needs to be given by the user, as the stope height will also dictate the mining level. A shorter stope will generate many levels and further impact the need for mine access while also creating the opportunity to do selective mining. On the contrary, a higher stope will generate fewer levels, but the production rate could be higher, further impacting the production cost. This condition is displayed in Fig. 2 where the stope's origin, positioned at the lowest elevation of the block model (marked by the green-colored box), is the determining block for the stope's height constraint ($ez_{i,j,k}$), which also defines the number and location of levels. Nevertheless, the final layout will be driven by the rock conditions, as this constraint only enforces one of the three axes.

In the proposed algorithm, the stope shape is controlled via block quantity relative to its axis. Thus, conversion from allowable stope height to allowable mining block is needed. Equation (4) implies that the maximum stope height is converted by dividing the maximum height by the block height. The calculation was possible because of the regularity of the block size.

$$ez_{i,j,k} = Hmax/Hb \quad (4)$$

2.3 Maximum and Minimum Width Constraint

The maximum and minimum constraints limit the stope size during the optimization process, ensuring that the optimal stope meets operational and geomechanical criteria. The dimensions of mining equipment are considered the minimum operational width defined by the user (W_{MIN}). The stope's width should accommodate the equipment size operating in that area. The use of mechanical equipment tends to require a larger minimum width for the stope compared to traditional mining. In some cases within narrow veins, the equipment width may conflict with the vein width, necessitating a wider stope to compensate for the mechanized mining activities in that location, further impacting the increase in planned dilution, thus reducing the economic feasibility of the stope.

Table 1 List of notations for the mathematical models and methodology

Symbol	Descriptions
Notations	
I	Index position of x
J	Index position of y
K	Index position of z
Parameters	
Ar	Factors A Mathews stability graphs in block
Br	Factors B Mathews stability graphs in block
Cr	Factors C Mathews stability graphs in block
Dr	Rock density
gr	Metal grade in block
gs	Metal grade in stope
$Hmax$	Maximum stope height
Hr	Block height
$HR1r$	Hydraulic radius on the 1-th wall of the stope
$HR2r$	Hydraulic radius on the 2-th wall of the stope
$HR3r$	Hydraulic radius on the 3-th wall of the stope
$HR4r$	Hydraulic radius on the 4-th wall of the stope
$Lmax$	Maximum length of stope determined by user
$Lmin$	Minimum length of stope determined by user
Lr	Block length
mr	Metal weight in block
ms	Metal weight in stope
$N1r$	N number on the 1-th wall of the stope
$N2r$	N number on the 2-th wall of the stope
$N3r$	N number on the 3-th wall of the stope
$N4r$	N number on the 4-th wall of the stope
ni	Number of blocks in x-direction
nj	Number of blocks in y-direction
nk	Number of blocks in z-direction
nxs	N-blocks towards x are allowed on the stope
nys	N-blocks towards y are allowed on the stope
nzs	N-blocks towards z are allowed on the stope
Qr	Q' value Q-system in block
tr	Ore tonnage in block
ts	Ore tonnage in stope
vs	Stope economic value
Wr	Block width
$Wmin$	Minimum width of stope determined by user
$Wmax$	Maximum width of stope determined by the user
Decision variables	
$tagr$	Tag for ore block
$Tags$	Tag for ore block in stopes
Ts	Positive stope tag database
Fs	Optimum stope tag database

Differing from the minimum width ($Wmin$), the minimum stope length ($Lmin$) is typically determined based on the length of the stope advancement, where its width is no smaller than the minimum stope advancement length. This constraint ensures that no stope design is created smaller than the stope advance length.

A significant factor affecting the maximum stope width and length ($Wmax$ and $Lmax$) is geomechanics. Solid rock, limited water presence, and favorable stress conditions are indicators of favorable rock conditions where stope sizes can generally be larger to meet production needs. Furthermore, in the design aspect, the orientation of the structure and stope walls can be a determining factor for stability/safety in stope design. Mathews [42] proposed an empirical approach applicable to open stopes or sublevel stoping, where the hydraulic radius and stability number (N') are used as indicators for the maximum stable stope dimensions. The application and integration of the geomechanical constraint model into the stope dimension constraints are explained in more detail in Section 4.

Geomechanical constraints are established by ensuring that the stopes have dimensions smaller than the allowed hydraulic radius at the location where the stopes will be formed. Meanwhile, operational constraints ensure that the dimensions of the stopes are larger than the minimum allowed dimensions at a block model location. Both of these constraints are combined in a unified constraint that regulates the maximum and minimum dimensions along the x-axis ($nxs_{i,j,k}$), y-axis ($nys_{i,j,k}$), and z-axis ($nzs_{i,j,k}$). The stope size is limited by Eq. (5) to (6), which add up the indices of the mined blocks ($tags$) in the stope layout and compare them to the stope size limits. Equations (5), (6), and (7), respectively, operate on the x-axis, y-axis, and z-axis.

$$nxs_{i,j,k} \geq \sum_{i=1}^{I}\sum_{j=1}^{J}\sum_{k=1}^{K} tags \forall i \in \{1 \ldots I\}, j \in \{1 \ldots J\}, k \in \{1 \ldots K\} \tag{5}$$

$$nys_{i,j,k} \geq \sum_{i=1}^{I}\sum_{j=1}^{J}\sum_{k=1}^{K} tags \forall i \in \{1 \ldots I\}, j \in \{1 \ldots J\}, k \in \{1 \ldots K\} \tag{6}$$

$$nzs_{i,j,k} \geq \sum_{i=1}^{I}\sum_{j=1}^{J}\sum_{k=1}^{K} tags \forall i \in \{1 \ldots I\}, j \in \{1 \ldots J\}, k \in \{1 \ldots K\} \tag{7}$$

The application of these equations serves as a constraint in the stope optimization phase, as depicted in Fig. 3. The green-colored blocks depict the block origin's position where the stope dimension constraints are applied, while the dashed red lines represent the boundary of the stope layout's location with the application of stope dimension constraints. With the integrated application of geomechanical considerations in the stope dimension constraint at each stope location, the stope dimensions can be deemed representative as they meet the rock conditions.

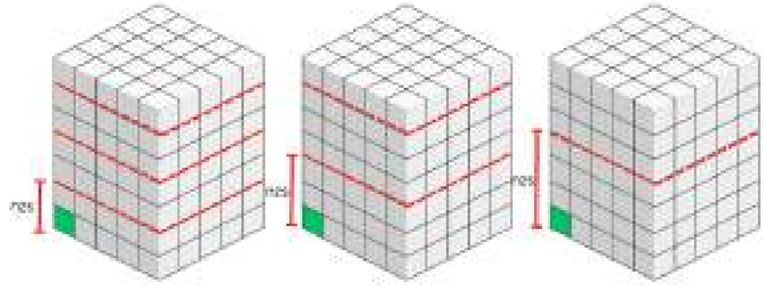

Fig. 2 Stope height constraint

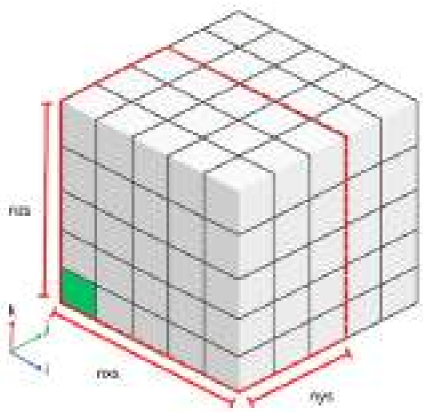

Fig. 3 Stope dimension constraint

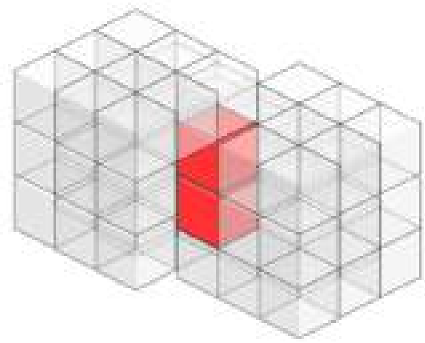

Fig. 4 Overlapping stopes

2.4 Stope Overlapping Constraint

"Overlapping stopes" is a condition where the optimized stope layouts intersect with each other [33]. This condition arises due to the formation of another optimal stope shape in a nearby location. Overlapping stope results in repeated calculations of volume and tonnage, which then raises the value of the mined material and leads to an overly optimistic assessment of the project's feasibility. Figure 4 depicts an illustration of overlapping stopes where the red-colored blocks represent the area where both stopes intersect. In this case, the material attributes within the red blocks will be counted twice, potentially resulting in inaccurate mined material and economic calculations for both stopes.

In this study, the overlap constraint is applied by utilizing the mined block index (mgs) assigned to each block falling within a stope. The stope layout is deemed feasible when, during stope determination, all blocks within that stope have a mined block index (mgs) equal to 0. This constraint application ensures that no stope can form in that location if even a single block has a mined block index (mgs) equal to one. Equation (8) shows the mathematical form of the stope overlap constraint, where $mgs_{i,j,k}$ is the mined block indexes.

$$fol_{i,j,k} = \begin{cases} 0 \text{ if } mgs_{i=1,j=1,k=1}^{i+nxs_{i,j,k},\, j+nys_{i,j,k},\, k+nzs_{i,j,k}} \geq 1 \\ 1 \text{ otherwise} \end{cases} \forall i \in \{1 \ldots I\}, j \in \{1 \ldots J\}, k \in \{1 \ldots K\} \quad (8)$$

3 Maximum Width and Span by Mathews Stability Chart

3.1 Mathews Stability Chart

Mathews [42] introduced a stability graph based on 26 cases collected from open-stope underground mining. This data was later supplemented and recalibrated by Potvin [43], which became widely used in the industry as the basis for stope planning that considers rock geomechanics conditions. The stability graph represents a plot of the stability number (N') against the shape factor (S) or also known as the hydraulic radius (HR). The calculation of N' is done by considering Rock Quality Designation (RQD), joint set number (J_n), joint roughness number (J_r), joint alteration number (J_a), stress factor (A), joint orientation factor (B), and gravity factor (C) through Eq. (9). Meanwhile, HR is generally the ratio between the area and the perimeter, which is determined based on the length (L) and width (W) of the stope, as shown in Eq. (10). Both of these variable results are plotted on the stability graph to determine the stability condition of the wall through three zones depicted on the graph: stable, unstable, and cave, as seen in Fig. 5.

$$N' = \left(\frac{RQD}{J_n}\right) \times \left(\frac{J_r}{J_a}\right) \times A \times B \times C \tag{9}$$

$$HR = \frac{W \times L}{2 \times (W \times L)} \tag{10}$$

This study employs the stability graph developed by Potvin [43] and Nickson [44] as a stability analysis tool within

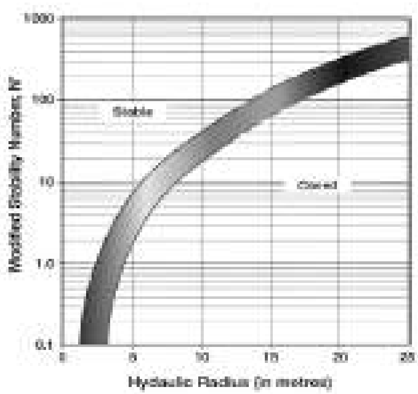

Fig. 5 Potvin-modified Mathews stability graphs [43]

the optimization algorithm. Equation (11) represents the boundary between the stable and unstable areas on the stability graph which was statistically calculated by Nickson [44] based on 175 case studies of stope stability in Potvin [43]. The stope wall dimensions allowed fall within the area above this boundary line. Through the use of this stability graph, it is also assumed that the stopes used in this algorithm are unsupported.

$$HR = 10^{(0.573+0.338\log N')} \tag{11}$$

3.2 Mathews Stability Chart Application in Stope Dimensional Constraint

In this study, improvements to the existing stope optimization algorithm were made by incorporating stability analysis using Mathews Stability Chart into the algorithm as dimensional constraints. Thus, the proposed algorithm has the ability to directly address rock conditions. This was done by assessing the Mathews attribute data provided in the block model. The analysis is conducted at block locations by iterating steps as follows:

1. Assessing the maximum of each stope wall domain by looking for the ore domain.
2. Calculate the *N stability number* based on *Q'* value, *factor A*, *factor B*, and *factor C* within the wall domain.
3. Determine the stable condition for the wall domain by correlating the hydraulic radius and the *N stability number*.
4. Assessing a smaller domain until a stable condition is met
5. Determine the allowable stope wall dimensions by choosing the lowest hydraulic conditions between each wall.

The algorithm steps are handled by several equations, as follows: Eqs. (12) and (13) are used for the first step, to determine which part of the rock is the ore body, so that subsequent iterations of the equation will be limited to the controlled by the *i*, *j*, and *k* indices of the block. The difference between the two equations lies in the orientation in which each equation is applied. Equation (12) is utilized on the stope wall oriented towards the east, while Eq. (13) is applied on the stope wall oriented towards the north. The calculation of the *N stability number* in the second step is performed by utilizing Eqs. (14) to (17). Each of the equations represents the different calculations performed for the four walls. As seen in the equations, all four equations have different block location indices, representing calculations for block data in different domains of the stope walls. The *N stability number* for each of the stope wall domains is then used to calculate the allowable *hydraulic* *radius* for the corresponding stope wall via Eqs. (18) to (21). Each of the *hydraulic radius* equations corresponds to the wall where it belongs, as the indices specifically emphasize where the calculation is performed.

$$ssr_{i,j,k} = \sum_{i=1}^{\ldots} \sum_{j=1}^{J} \sum_{k=1}^{K} ssp \; \forall i \in \{1 \ldots I\}, j \in \{1 \ldots J\}, k \in \{1 \ldots K\} \quad (12)$$

$$sru_{i,j,k} = \sum_{i=1}^{I} \sum_{j=1}^{\ldots} \sum_{k=1}^{K} sup \; \forall i \in \{1 \ldots I\}, j \in \{1 \ldots J\}, k \in \{1 \ldots K\} \quad (13)$$

$$N1r_{i,j,k} = MINNr_{\ldots} \; \forall i \in \{1 \ldots I\}, j \in \{1 \ldots J\}, k \in \{1 \ldots K\} \quad (14)$$

$$N2r_{i,j,k} = MINNr_{\ldots} \; \forall i \in \{1 \ldots I\}, j \in \{1 \ldots J\}, k \in \{1 \ldots K\} \quad (15)$$

$$N3r_{i,j,k} = MINNr_{\ldots} \; \forall i \in \{1 \ldots I\}, j \in \{1 \ldots J\}, k \in \{1 \ldots K\} \quad (16)$$

$$N4r_{i,j,k} = MINNr_{\ldots} \; \forall i \in \{1 \ldots I\}, j \in \{1 \ldots J\}, k \in \{1 \ldots K\} \quad (17)$$

$$HR1r_{i,j,k} = 10^{0.573+0.338\log(N1r_{i,j,k})} \; \forall i \in \{1 \ldots I\}, j \in \{1 \ldots J\}, k \in \{1 \ldots K\} \quad (18)$$

$$HR2r_{i,j,k} = 10^{0.573+0.380\log(N2r_{i,j,k})} \; \forall i \in \{1 \ldots I\}, j \in \{1 \ldots J\}, k \in \{1 \ldots K\} \quad (19)$$

$$HR3r_{i,j,k} = 10^{0.573+0.380\log(N3r_{i,j,k})} \; \forall i \in \{1 \ldots I\}, j \in \{1 \ldots J\}, k \in \{1 \ldots K\} \quad (20)$$

$$HR4r_{i,j,k} = 10^{0.573+0.380\log(N4r_{i,j,k})} \; \forall i \in \{1 \ldots I\}, j \in \{1 \ldots J\}, k \in \{1 \ldots K\} \quad (21)$$

The selection of the lowest hydraulic radius is then performed on opposing walls to ensure that the lowest value to be used is indicated by Eqs. (22) and (23). The allowable length for stope walls is then determined based on the *hydraulic radius* of the corresponding wall through Eqs. (24) and (25). In the last stage, Eqs. (26) and (27) are making sure that the allowable length for the stope wall has already met operational constraints.

$$HR1r_{i,j,k} = \begin{cases} HR1r_{i,j,k} \text{ if } HR1r_{i,j,k} < HR2r_{i,j,k} \\ HR2r_{i,j,k} \text{ otherwise} \end{cases} \; \forall i \in \{1 \ldots I\}, j \in \{1 \ldots J\}, k \in \{1 \ldots K\} \quad (22)$$

$$HR3r_{i,j,k} = \begin{cases} HR1r_{i,j,k} \text{ if } HR3r_{i,j,k} < HR4r_{i,j,k} \\ HR4r_{i,j,k} \text{ otherwise} \end{cases} \; \forall i \in \{1 \ldots I\}, j \in \{1 \ldots J\}, k \in \{1 \ldots K\} \quad (23)$$

$$wsl_{i,j,k} = \frac{2HR1r_{i,j,k} \times wsl_{i,j,k} \times Hn_{i,j,k}}{(wsl_{i,j,k} \times Hn_{i,j,k}) - 2HR1r_{i,j,k}} \times Ln_{i,j,k} \; \forall i \in \{1 \ldots I\}, j \in \{1 \ldots J\}, k \in \{1 \ldots K\} \quad (24)$$

$$mcs1_{i,j,k} = \frac{2HCSr_{i,j,k} \times r_{i,j,k} \times Ha_{i,j,k}}{(ucs_{i,j,k} \times Ha_{i,j,k}) - 2HCSr_{i,j,k}} \times La_{i,j,k} \forall i \in \{1 \ldots I\}, j \in \{1 \ldots J\}, k \in \{1 \ldots K\} \tag{25}$$

$$mcs_{i,j,k} \begin{cases} 0 \; if \; mcs_{i,j,k} > \frac{Lmax}{La} \\ mcs1_{i,j,k} \; if \; mcs_{i,j,k} > mcs1_{i,j,k} > \frac{Lmin}{La} \\ mcs_{i,j,k} \; otherwise \end{cases} \forall i \in \{1 \ldots I\}, j \in \{1 \ldots J\}, k \in \{1 \ldots K\} \tag{26}$$

$$mcs_{i,j,k} \begin{cases} 0 \; if \; mcs_{i,j,k} > \frac{Hmax}{La} \\ mcs1_{i,j,k} \; if \; mcs_{i,j,k} > mcs1_{i,j,k} > \frac{Hmin}{La} \\ mcs_{i,j,k} \; otherwise \end{cases} \forall i \in \{1 \ldots I\}, j \in \{1 \ldots J\}, k \in \{1 \ldots K\} \tag{27}$$

4 Optimization

Nhelko A [45] emphasizes the limitations of exact algorithm application in large-scale cases such as stope optimization. Although the resulting solutions may achieve the global optimum, the problem-solving time typically increases exponentially with problem complexity, making this algorithm category infeasible for large-scale cases. Heuristic algorithms are commonly employed solutions for addressing complex problems like stope optimization, ensuring fast problem-solving while still focusing on optimization objectives. This study applies heuristic algorithms in optimization techniques, enabling large-scale cases to serve as a benchmark for algorithm validation. One of the previously developed heuristic algorithms is Sandanayake [29, 31]. Sandanayake [29] introduces a heuristic algorithm for stope optimization with the following general steps:

1. Initialization of all data, parameters, and variables
2. Stope formation through mining block aggregation
3. Update of stope attributes based on mined blocks
4. Extraction of subsets with economic values greater than 0
5. Identification of overlapping stopes
6. Creation of a set containing non-overlapping stopes
7. Calculation of economic value for each non-overlapping stope set
8. Selection of sets and determination of stopes with the highest economic value.

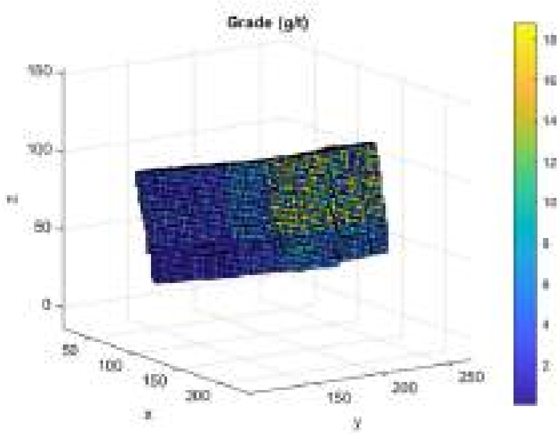

Fig. 6 Block model for Au grade

The algorithm was modified by incorporating Mathews' stability considerations into the stope dimension constraints (σ_{yz}, σ_{xz}, σ_{xy}). The varying dimension constraints are held by each block within the block model in line with the geomechanical conditions of that block. Hence, the stope dimensions will vary according to the geomechanical conditions at that location. These constraint applications are implemented in the initial stage of stope creation. The subsequent stage remains relevant, where non-overlapping stopes are created, and ultimately, the stope set with the highest economic value is selected.

5 Case Study

To test the validity of the algorithm proposed in this study, a block model was created by considering several case studies of underground gold mines in Indonesia. Prasetyo et al. [46] modeled a gold vein deposit at one of the mines in Indonesia using the fractal method and compared it to the classical method. In that study, the gold and silver reserves were divided into two zones that were delimited at an elevation of 500 m above sea level. Another study [47] provided an overview of rock mass classes at some underground mines with narrow vein ore types in Indonesia, which were dominated by moderate-to-weak rock. The block model was then created to represent the same conditions.

5.1 The Block Model

Figure 6 explains the uniform dimension block model created from the minimum and maximum ranges of easting, northing, and elevation, respectively, of 100, 100, 35 to 145, 267.5, 102.5. The number of blocks on the x, y, and z axes is 18, 67, and 27, respectively, so the total block model is 32,562. The rock density is set at 2.36 tons/m^3, while the gold grade in the block is divided into six zones, namely upper-high, upper-mid, upper-low, lower-high, lower-mid, and lower-low. The upper and lower zones are separated at an elevation of 60 m above sea level, while the high and mid zones and the mid and low zones are separated at a northing of 210 and 150, respectively. The gold grade in each zone was then created using Eq. (28), where the base grade for each zone (upper-high, upper-mid, upper-low, lower-high, lower-mid, lower-low) is 18.8 g/t, 9.4 g/t, 4.7 g/t, 9.9 g/t, 4.9 g/t, and 2.5 g/t. To better represent the real condition, a random number is introduce to randomize the base. Additionally, Table 2 shows the economic parameters used in the block's economic calculation.

The same method is applied to the creation of Q' values in the block model. The Q' model is not divided into upper and lower zones but only into high, mid, and low zones that are delimited by the same northing as previously described. Equation (29) explains how the Q' value is created in the block model, where the Q' base in the high, mid, and low zones is set to 10.1, 1.1, and 2.7, respectively. Sulistianto et al. [48] determined the rock mass class conditions at one of the underground gold mines in Indonesia, which was used as a basis for the value of 0.5 for factors A and B. Factor C is set to 8 because the assessment in this algorithm is only done on the stope walls that have a vertical orientation.

Table 2 Economic parameter

Parameter	Value
Metal price ($/gram)	54.8
Mining cost ($/ton)	35.8
Processing cost ($/ton)	1.6
Refining cost ($/ton)	3.9
Global recovery (%)	80

$$AuGrade = randomnumber \times Augradebase \tag{28}$$

$$Q' = randomnumber \times Q'base \tag{29}$$

5.2 The Test Methodology

A number of scenarios are used to see the performance of the Mathews analysis in the algorithm that can produce the stope dimension variable in the algorithm. In this validation, three scenarios are used, including the fixed maximum stope dimension, the fixed minimum stope dimension, and the proposed algorithm, which are subsequently referred to as scenarios 1, 2, and 3. The three scenarios were created to explore the optimization potential of stopes with varied shapes due to the variations in rock conditions compared to the commonly practiced optimization based on fixed dimensions. Scenarios 1 and 2 represent optimization with fixed dimensions, while scenario 3 represents stopes with varied. Nevertheless, to enable a comparison between scenarios, the stope height for each scenario is set at 5 m.

In scenario 1, the stope dimension is set according to the maximum dimension allowed based on best geomechanical conditions found in the block model data. The calculations are performed based on the N' value for the best rock condition found in the block model. The largest dimension is determined by calculating the HR value for that rock condition. Because the stope height is fixed, the width (l) and length (w) of the stope can be determined. It is known that

Table 3 Validation scenarios

Scenario	Stope dimension ($l \times w \times h$) (m)
Scenario 1	7.5 × 7.5 × 5
Scenario 2	5 × 5 × 5
Scenario 3	Variable

Table 4 Optimization results

Parameter	Scenario 1	Scenario 2	Scenario 3
Number of stopes	195	711	302
Mined tonnage (ton)	238,777	214,161	165,658
Mined metal (grams)	864,736	940,086	856,880
Mined average grade (g/t)	3.62	4.40	5.17
Economic value ($)	26,283,967	30,640,495	28,700,093

the width and length of the stope based on the rock condition in the block model are 7.5 m. Compared to scenario 1, the minimum stope width and length allowed in scenario 2 is based on operational considerations set at 5 m. This minimum dimension is also applied in scenario 3 as the basis for achieving operational considerations in the optimization phase. The optimization application based on geomechanical considerations is manifested in scenario 3, where the algorithm is given the freedom to determine stope dimensions according to the geological, economic, and geomechanical considerations available in the block model. The scenarios in this case study are seen in Table 3.

To assess the validity of stability analysis application within the stope optimization algorithm, a validation was conducted through back analysis on the final stope walls. Analysis on all four stope walls was carried out by plotting the hydraulic radius (*HR*) of the stope wall against the stability number (*N'*). The optimization results can be considered valid if all plots of the stope walls fall within the stable zone. Further details are provided in Section 8.

6 Results

Table 4 shows the results of the optimization in the three scenarios, while the results of the stopes that have been optimized are shown in Fig. 7. From Table 4, it can be seen that the integration of the Mathews stability module into the algorithm

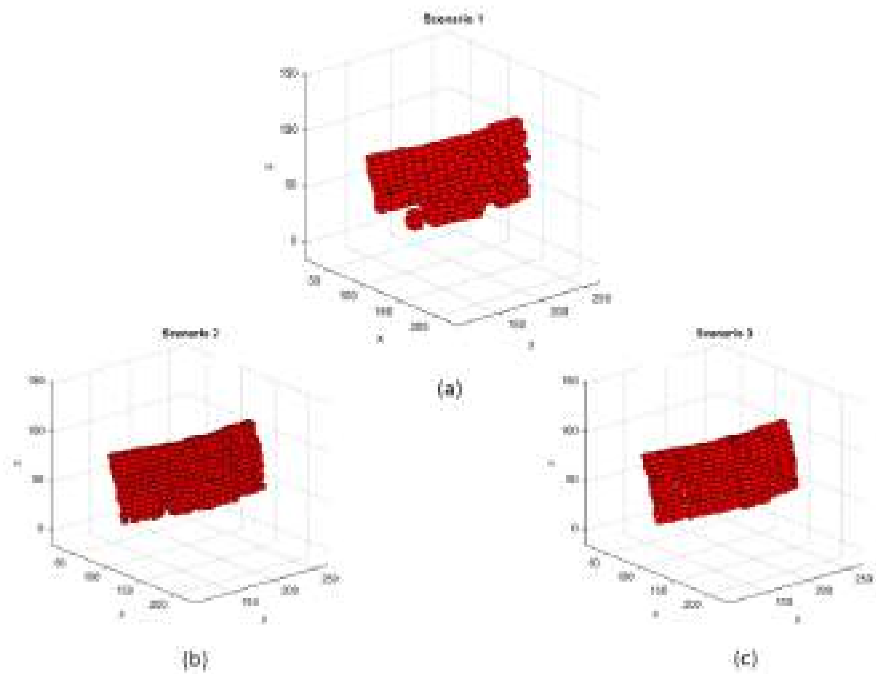

Fig. 7 **a–c** Optimized stopes

in scenario 3 has a level of economy that is competitive with the optimization of the fixed dimension stopes. In general, the varied shape of the stope, following the ore shape, provides an advantage in minimizing mined material waste, as indicated by the highest mined grade among the three scenarios. Furthermore, mining can be considered more efficient. The smaller amount of mined material in scenario 3 indicates that there is less material to be moved for a higher economic value.

In scenario 2, however, the value of the stopes is higher than in scenario 3, which is considered normal for optimization to be carried out on the same cost components in each scenario. As optimization is carried out on the same cost basis across all scenarios, the results will tend towards smaller dimensioned stopes as they can maximize the reserves. In actual case studies, smaller stopes can lead to lower productivity, resulting in relatively smaller economic value due to higher mining costs. The further relationship between the dimensions and the cost of the stopes needs to be established for the algorithm to perform better.

Figure 7 shows the visualization of the optimized stope in all three scenarios. Scenario 1 is unable to maximize the reserves in areas with low grades because the large stope size causes a lot of mined waste material, so the profit from mining ore must compensate for this. This condition is visible in Fig. 7a at low elevations in the southern part, where no stopes are formed in those locations, indicating stopes with negative economic value. In contrast, scenario 2 (Fig. 7b) and scenario 3 (Fig. 7c) showed the opposite results, where the smaller stope dimensions in scenario 2 were able to accommodate ore grade variations better, while the flexibility in dimension selection in scenario 3 had the same effect.

7 Stability Confirmation with Mathews

Validation of stope stability was performed on each final stope wall formed in scenario 3. The stability number (S) values for each wall were plotted against the corresponding hydraulic radius (HR) values of the stope wall to determine the stability condition of each wall using Mathews' stability graph. Based on the back analysis plots conducted, all of the optimized stope walls have stable conditions, as indicated by the stability points plotted above the stability line in Fig. 3. In the hanging wall and footwall areas, all stope walls can be considered stable, as seen in Fig. 8 (left). The distribution of the plots tends to be vertical, indicating variations in the rock conditions within the block model, while the tight horizontal distribution indicates consistent stope wall areas. A similar pattern is observed in the distribution of plots for the front wall and back wall (Fig. 8 (right)), suggesting a similar condition in those areas. The tight horizontal distribution also indicates minimal variations in the length or width of the formed stopes, which is commonly observed in narrow deposit formations as utilized in this case study. Further, the application of the Mathews stability analysis to the optimization algorithm was deemed successful, as indicated by the good stope economic values and stable conditions at each stope wall.

8 Conclusions

One of the significant challenges in underground mine planning is determining the stope layout, which involves the location, wall area, and stope size. The stope layout

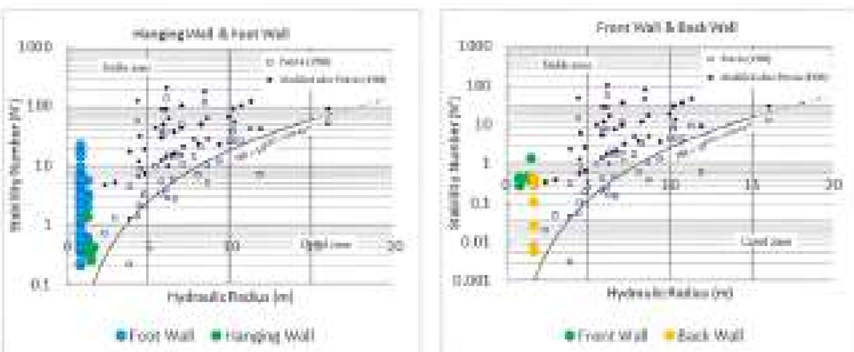

Fig. 8 Stability analysis for optimized stope wall

dictates the amount of material extracted, the metal content, and grade of minerals extracted, ultimately determining the aggregate economic value of all extracted stopes. Addressing this challenge has been largely done through the development of optimization algorithms, enabling mining engineers to assess various stope layouts more efficiently. However, the involvement of numerous parameters renders optimization algorithms susceptible to suboptimal conditions, wherein the stope layout produced by the optimization process may not be the best solution achievable for a given case study. Among the multitude of parameters involved, rock conditions are one of the dominant parameters considered in determining the stope layout. The study's proposed algorithm tried to combine the steps of stope optimization with stability analysis using the Mathews Stability Chart. This was done so that a more complete design could be made, especially since more field data about the geomechanical properties was available.

Integration is suggested by establishing dimensional constraint at the onset of optimization utilizing Mathews stability analysis. This involves incorporating geomechanical data, such as rock mass classification Q', factor A, factor B, and factor C. The outcomes demonstrate the effectiveness of this approach, evident in the optimization outcomes that yield superior economic value compared to employing fixed dimensions. Furthermore, the stability of the optimized stope walls affirms the effectiveness of stability analysis within the optimization algorithm, ensuring the project's financial feasibility. The results of optimization by this algorithm could serve as preliminary guidance for mine planners during the feasibility evaluation phase.

Author Contribution Conceptualization, software, investigation, visualization, writing—review and editing, and project administration: Dana Putra; methodology, validation, formal analysis, and writing—review and editing: Tri Karian; validation, resources, writing—review and editing, supervision, and funding acquisition: Budi Sulistianto; supervision, resources, validation, and writing—review and editing: Mohamad Nur Heriawan.

Funding The authors express great appreciation to Institut Teknologi Bandung through the Riset Unggulan ITB 2022 for funding this study.

Data Availability The data that support the findings of this study are available from the corresponding author upon reasonable request.

Declarations

Competing Interests The authors declare no competing interests.

References

1. Mawdesley C, Trueman R, Whiten WJ (2001) Extending the Mathews stability graph for open–stope design. Min Technol 110:27–39. https://doi.org/10.1179/mnt.2001.110.1.27
2. Lu A, Yin C, Zhang N (2019) Analytic stress solutions for a lined circular tunnel under frictional slip contact conditions. Eur J Mech A Solids 75:11–20. https://doi.org/10.1016/J.EUROMECHSOL.2019.01.008
3. Vitali OPM, Celestino TB, Bobet A (2019) Shallow tunnels misaligned with geostatic principal stress directions: analytical solution and 3d face effects. Tunn Undergr Space Technol 89:268–283. https://doi.org/10.1016/J.TUST.2019.04.006
4. Napa-García GF, Câmara TR, and Navarro Torres VF (2019) Optimization of room-and-pillar dimensions using automated numerical models. Int J Min Sci Technol 29. https://doi.org/10.1016/J.IJMST.2019.02.013
5. Abdellah WR, Ahmed HM, Hefni MA (2019) Numerical modelling of staged stope extraction in a tabular steeply dipping deposit. Geomech Geoeng 14:41–51. https://doi.org/10.1080/17486025.2018.1508856
6. Mirzaah T (2023) A binary integer linear programming model for optimizing a binary integer linear programming model for optimizing underground stope layout underground stope layout. https://scholarsmine.mst.edu/masters_theses/8176
7. Lowson AR, Bieniawski ZT (2013) Critical assessment of RMR based tunnel design practices: a practical engineer's approach. SME
8. Kang Z et al (2019) Optimization calculation of stope structure parameters based on Mathews stabilization graph method. J Vibroeng 21:1227–1239
9. Wang D et al (2021) Stope stability assessment by the Mathews-Potvin method: a case-study of open stoping in salt rock mass under conditions of secondary stress field. IOP Publishing. https://doi.org/10.1088/1755-1315/684/1/012011
10. Liu H, Zhao Y, Zhang P, Liu F, Yang T (2021) Stope structure evaluation based on the damage model driven by microseismic data and Mathews stability diagram method in Xiadian gold mine. Geomat Nat Haz Risk 12:1616–1637. https://doi.org/10.1080/19475705.2021.1941308
11. Jaroszewski M, Prattow S, Rimac M (2021) Industry survey on the current state of stope design methods in the underground mining sector. Energies (Basel) 15:240. https://doi.org/10.3390/en15010240
12. Nikbin V, Ataee-pour M, Shahriar K, Pourrahimian Y, MirHassani SA (2019) Stope boundary optimization: a mathematical model and efficient heuristics. Resour Policy 62:515–526. https://doi.org/10.1016/J.RESOURPOL.2018.10.007
13. Bashri Z (2018) Stopes layout and production scheduling optimization in sublevel stoping mining. Dissertation, University of Alberta
14. Nelis G, Gamache M, Marcotte D, Bai X (2016) Stope optimization with vertical convexity constraints. Optim Eng 17:813–832. https://doi.org/10.1007/s11081-016-9321-6
15. Wilson B (2020) Heuristic stochastic stope layout optimization. University of Alberta. Thesis
16. Furtado e Faria M, Dimitrakopoulos R, and Lopes Pinto CL (2022) Integrated stochastic optimization of stope design and long-term underground mine production scheduling. Resources Policy 78. https://doi.org/10.1016/j.resourpol.2022.102918.
17. Furtado e Faria MA, Dimitrakopoulos R, Pinto C (2022) Stochastic stope design optimisation under grade uncertainty and dynamic development costs. Int J Min Reclam Environ 36:81–103. https://doi.org/10.1080/17480930.2021.1968707

18. Sari YA, Kumral M (2021) Sublevel stope layout planning through a greedy heuristic approach based on dynamic programming. J Oper Res Soc 72:554–563. https://doi.org/10.1080/01605682.2019.1700179
19. Tolouei K, Moosavi E, Tabrizi AHB, Afzal P, Bazzazi AA (2021) An optimisation approach for uncertainty-based long-term production scheduling in open-pit mines using meta-heuristic algorithms. Int J Min Reclam Environ 35:115–140. https://doi.org/10.1080/17480930.2020.1773119
20. Lamghari A, Dimitrakopoulos R (2020) Hyper-heuristic approaches for strategic mine planning under uncertainty. Comput Oper Res 115:104590. https://doi.org/10.1016/j.cor.2018.11.010
21. Ovanic J, Young DS (1995) Economic optimisation of stope geometry using separable programming with special branch and bound techniques. McGill University
22. Riddle JM (1977) Dynamic programming solution of a block-caving mine layout. 767–780. https://www.onemine.org/documents/a-dynamic-programming-solution-of-a-block-caving-mine-layout Accessed: Jan. 20, 2023
23. Deraisme J, De Fouquet C, Fraisse H (1984) Geostatistical orebody model computer optimization of profits from different underground mining methods. 583–590
24. Cheimanoff NM, Deliac EP, Mallet JL (1989) GEOCAD: an alternative cad and artificial intelligence tool that helps moving from geological resources to mineable reserves. Publ by Soc of Mining Engineers of AIME
25. Alford C (1995) Optimisation in underground mine design.
26. Cawrse I (2001) Multiple pass floating stope process.
27. Ataee-Pour M (2004) Optimisation of stope limits using a heuristic approach. Inst Mining Metall Trans Sect A. Min Technol 113: https://doi.org/10.1179/037178404225004959.
28. Topal E, Sens J (2010) A new algorithm for stope boundary optimization. J Coal Sci Eng 16:113–119. https://doi.org/10.1007/s12404-010-0201-y
29. Sandanayake DSS, Topal E, Ali Asad MW (2015) A heuristic approach to optimal design of an underground mine stope layout. Appl Soft Comput 30:595–603. https://doi.org/10.1016/J.ASOC.2015.01.060
30. Bai X, Marcotte D, Simon R (2013) Underground stope optimization with network flow method. Comput Geosci 52:361–371. https://doi.org/10.1016/j.cageo.2012.10.020
31. Sandanayake DSS, Topal E, Asad MWA (2015) Designing an optimal stope layout for underground mining based on a heuristic algorithm. Int J Min Sci Technol 25:767–772. https://doi.org/10.1016/j.ijmst.2015.07.011
32. Sandanayake DSS (2014) Stope boundary optimisation in underground mining based on a heuristic approach. Dissertation, Curtin University
33. Sari YA, Kumral M (2019) A planning approach for polymetallic mines using a sublevel stoping technique with pillars and ultimate stope limits. Eng Optim 52:932–944. https://doi.org/10.1080/0305215X.2019.1624739
34. Sari YA, Kumral M (2021) Clustering-based iterative approach to stope layout optimization for sublevel stoping. J South Afr Inst Min Metall 121:93–100. https://doi.org/10.17159/2411-9717/1237/2021
35. Kumral M, Sari YA (2020) Underground mine planning for stope-based methods. AIP Publishing LLC 10(1063/5):0006787
36. Villalba Matamoros ME, Kumral M (2017) Heuristic stope layout optimisation accounting for variable stope dimensions and dilution management. Int J Min Miner Eng 8:1–18. https://doi.org/10.1504/IJMME.2017.082680
37. Hou J, Xu C, Dowd PA, Li G (2019) Integrated optimisation of stope boundary and access layout for underground mining operations. Min Technol 128:193–205. https://doi.org/10.1080/25726668.2019.1603928
38. Y Nikbin E Mardaneh M Waqar A Asad E Topal 2021 Pattern search method for accelerating stope boundary optimization problem in underground mining operations https://doi.org/10.1080/0305215X.2021.1932869
39. Erdogan A, Hamidi JK, Monjezi A (2023) Determination of sublevel stoping layout using a network flow algorithm and the MRMR classification system. Resour Policy 80:103265. https://doi.org/10.1016/J.RESOURPOL.2022.103265
40. Laubscher DH (1990) A geomechanics classification system for the rating of rock mass in mine design. J South Afr Inst Min Metall 90:257–273
41. Potvin Y, Hadjigeorgiou J (2001) The stability graph method. Underground Mining Methods 66:513–520
42. Mathews, K. E. Hoek, D. C. Wyllie, and S. B. V. Stewart (1980) Prediction of stable excavation spans for mining at depths below 1000 metres in hard rock. https://www.scirp.org/(S(czeh2tfqyw2orz553k1w0r45))/reference/ReferencesPapers.aspx?ReferenceID=1059122 Accessed: Mar. 02, 2020
43. Potvin Y (1988) Empirical open stope design in Canada. University of British Columbia
44. Nickson SD (1992) Cable support guidelines for hard rock mine operations. University of British Columbia
45. Nikbin A, Tholana T, Nzingo P (2018) A review of underground stope boundary optimization algorithms. Resour Policy 56:59–69. https://doi.org/10.1016/J.RESOURPOL.2017.12.004
46. Prasetyo E (2010) Fractal model and classical block model in ore reserve estimation: a comparison. Riset Geologi Dan Pertambangan 20:119–130
47. Purwanto SH, Sasaoka T, Wattimena RK, Matsui K, Matsui K (2013) Influence of stope design on stability of hanging wall decline in Cibaliung underground gold mine. Int J Geosci 04:1–8. https://doi.org/10.4236/ijg.2013.410A001
48. Budi S, Wattimena RK, Arifianto A, Matsui K (2009) Determination of stope geometry in jointed rock mass at Pongkor underground gold mine. Int J JCRM 5:63–68. https://doi.org/10.11187/ijjcrm.5.63

Publisher's Note Springer Nature remains neutral with regard to jurisdictional claims in published maps and institutional affiliations.

Integration of Stability Factor A, B, and C on Mathews Stability Graph

ORIGINALITY REPORT

8%	7%	8%	3%
SIMILARITY INDEX	INTERNET SOURCES	PUBLICATIONS	STUDENT PAPERS

PRIMARY SOURCES

1	V. Nikbin, M. Ataee-pour, K. Shahriar, Y. Pourrahimian, S.A. MirHassani. "Stope boundary optimization: A mathematical model and efficient heuristics", Resources Policy, 2019 Publication	2%
2	www.sid.ir Internet Source	1%
3	escholarship.mcgill.ca Internet Source	1%
4	Yang Li, Nan Wang, Yifei Song, Xinghai Lei, Tiezheng Li, Lingyun Zou. "Quantitative Criterion and Applications for Assessing the Impact of Coal Seam Mining on Overlying Strata", Mining, Metallurgy & Exploration, 2024 Publication	1%
5	sites.ualberta.ca Internet Source	<1%
6	journal.ipb.ac.id Internet Source	<1%
7	www.db-thueringen.de Internet Source	<1%
8	repositorio.uchile.cl Internet Source	<1%
9	www.scribd.com Internet Source	<1%

10	www.tandfonline.com Internet Source	<1 %
11	Ahmadreza Esmaeili, Jafar Khademi Hamidi, Amin Mousavi. "Determination of sublevel stoping layout using a network flow algorithm and the MRMR classification system", Resources Policy, 2023 Publication	<1 %
12	Yan Zhang, Honglin Hu, Masayuki Fujise. "Resource, Mobility, and Security Management in Wireless Networks and Mobile Communications", Auerbach Publications, 2019 Publication	<1 %
13	A. Suarez. "A Comparative Evaluation of Different Versions Of the Strongly Implicit Procedure (SIP)", Proceedings of SPE Symposium on Numerical Simulation of Reservoir Performance NSS, 02/1976 Publication	<1 %
14	coek.info Internet Source	<1 %
15	pure.rug.nl Internet Source	<1 %

Exclude quotes	On	Exclude matches	< 15 words
Exclude bibliography	On		